https://doi.org/10.3311/PPci.37013

Periodica Polytechnica Civil Engineering

The Effect of Mineral Composition on the Correlation between Point Load Index with the Uniaxial Compressive Strength of Sulfate Rocks and their Point Loading Deformation

Mohammad Reza Rahimi[1], Seyed Davoud Mohammadi[1*]

[1] Department of Geology, Faculty of Science, Bu-Ali Sina University, Hamedan 6516738695, Iran
[*] Corresponding author, e-mail: d.mohammadi@basu.ac.ir

Received: 30 March 2024, Accepted: 15 May 2024, Published online: 10 July 2024

Abstract

Point load test is a common, inexpensive and fast test for the indirect achievement of compressive or tensile strength of the rocks in the laboratory and the field. In this research, by conducting uniaxial compression test (UCT), axial (APLT), and diametral (DPLT) point load tests on gathered sulfate rock blocks from the Gachsaran Formation outcrops at the four under-construction reservoir dam sites in Iran, investigate the effect of mineral composition on the relationships between point load index, the uniaxial compressive strength (UCS) and their point load deformation. Regarding that, firstly by creating a correlation between axial (APLI) and diametral (DPLI) point load index and UCS, relationships for each specific mineral composition were provided. Secondly, by comparing the reliability of the APLT and DPLT results in predicting UCS, the conversion factors of the APLI and DPLI to the UCS were calculated. Thirdly, the effect of unique or multiple sampling locations in the analysis results was compared, and finally, for the first time, the deformation of loading points in point load tests was investigated. The results of this study confirmed that by variation of mineral composition of sulfate rocks, the relationships between APLI and DPLI, and UCS, conversion factors as well as loading points deformation patterns during point load tests are changed significantly, and the results of APLT and DPLT can be used to predict UCS with the same reliability in dry and saturated conditions.

Keywords

the Gachsaran Formation, axial point load test, diametral point load test, deformation

1 Introduction

Point load strength test (PLST or PLT) is a common test in many rock engineering projects, and its method is described by standards such as ISRM [1] and ASTM D5731-16 [2]. PLT has been used as an efficient and practical method to evaluate the strength and classification of rock mass [3–8]. Point Load Strength Index (PLSI or PLI) has often been used as an indirect measure of rock's compressive or tensile strength [3, 5, 9, 10]. Doing a PLT is much easier and faster than a uniaxial compressive strength test (UCT), requires less preparation effort to sample and even lump samples can be used for testing and can be done quickly in the field and at the project site. This test can be performed in three types: axial, diametral and lump. In PLT, rock specimens (cylindrical, prismatic, or irregular) are placed between two contact points of coaxial, truncated conical platens, and then the load is applied at a constant rate so that the specimen can be failure in 10 to 60 seconds (The time specified in both of the mentioned standards). According to ISRM [1] and ASTM D5731-16 [2] standards, the test results are acceptable when the failure surface passes through two conical platen loading points. One of the most initial relationships that can be pointed between UCS and PLI (or I_s) is the D'Andrea et al.'s [9] equation for determining UCS using PLI:

$$\mathrm{UCS} = 15.3\ \mathrm{PLI} + 16.3. \tag{1}$$

Broch and Franklin [3] reported that the UCS of 50 mm diameter cores is approximately 24 times the PLI. They also provided a diagram to correct the sample size so that cores with different diameters could be used to determine the strength of the rock. Bieniawski [5] used a conversion factor k equal to 24 in his equation based on data from UCTs and PLTs on different types of rocks. However, Pells [11] showed that applying a conversion factor of 24

Cite this article as: Rahimi, M. R., Mohammadi, S. D. "The Effect of Mineral Composition on the Correlation between Point Load Index with the Uniaxial Compressive Strength of Sulfate Rocks and their Point Loading Deformation", Periodica Polytechnica Civil Engineering, 2024. https://doi.org/10.3311/PPci.37013

to the PLI for UCS estimation could lead to a 20% error in predicting the UCS of rocks such as dolerite, norite, and pyroxenite. Since the 1970s, the PLI of different rocks and their correlations with UCS have been studied by various researchers, and many experimental equations for relating PLI or $I_{s(50)}$ to UCS have been developed:

$$\mathrm{UCS} = k\ I_{s(50)}. \tag{2}$$

The value of the conversion factor (k) in the generalized linear Eq. (2) depends on the type of rock, its lithological, structural and engineering characteristics. As shown in Table 1 [1, 3, 5, 8, 9, 11–53], most of the relationships between $I_{s(50)}$ and UCS are linear, but some do not intersect at the origin of the coordinates, or some are power or nonlinear equations.

A review of the literature shows some kinds of sedimentary [5, 12–14, 17–19, 21, 25, 26, 28, 29, 31–33, 35, 36, 41, 48, 49, 53], metamorphic [35, 41, 42, 48–50] and igneous [12, 14, 23, 27, 35, 39, 51, 53] rocks have been investigated, and several relationships have been presented. Some researchers have also considered the effect of mineral composition on the correlation between PLI and UCS. Tuğrul and Zarif [30], by examining granite's physical and mechanical properties, showed a correlation between the mineral composition and the engineering strength properties of rock. Lindqvist et al. [54] investigated the effects of mineral composition, grain size, porosity and micro-cracks on the mechanical properties of rock. Ioanna et al. [55] have been shown a relationship between mineral composition and rock strength in weak rocks (types of marl such as calcareous marl and clay marl). Yusof and Zabidi [56] investigated the correlation between the mineral composition and textural properties of granite and engineering properties, including PLI, UCS and tensile strength. Although linear equations were presented between the mineral compositions and the three mentioned engineering strengths, but the presented equations had weak determination coefficients (for point load, $R^2 = 0.165$, for UCS, $R^2 = 0.378$, and for tensile strength, $R^2 = 0.39$). Li et al. [57] investigated the effect of mineral composition, microstructure and pore properties on the mechanical properties of four types of sandstone and stated that these properties are very closely related to the mechanical properties of the rock. Yasir et al. [58] investigated the effect of mineral composition of sandstone rocks on uniaxial compressive and point load strength and concluded that the alkali silica reactivity not really significant with the point load strength and uniaxial compression strength. Davarpanah et al. [59] studied the mechanical properties of dry, saturated, and frozen marls using destructive and non-destructive laboratory approaches and reported that there is linear correlation between uniaxial compressive strength and $I_{s(50)}$ in saturated, and frozen conditions with a determination coefficient of $R^2 = 0.74$ and $R^2 = 71$, respectively and a good correlation under dry condition with the determination coefficient 0.7 and the α value in the linear correlation relations was presented to −8.55, 3.73 and 6.52. Contact problem and pre-cracks in some materials have been investigated by many researchers. Yaylaci et al. [60–63], have been investigated the punching phenomena in soft and rigid materials and their contact problems. Yaylaci [64] and Yaylaci et al. [65] have been studied the effect of pre-crack on behavior of soft materials.

The correlation between $I_{s(50)}$ and UCS of gypsum rocks has also been considered by researchers such as Yılmaz and Yuksek [38] and Heidari et al. [44]. Yılmaz and Yuksek [38] reported a general relationship between the axial point load index and UCS. However, Heidari et al. [44] presented equations between axial, diametrical and lump point load indices with UCS for air-dried and saturated samples. Unfortunately, these researchers did not provide information on the mineral composition and texture of the studied gypsum rocks. The rock blocks used by Heidari et al. [44] were collected from the Gachsaran Formation outcrops in Iran, as in this study. The correlated relationships by all three researchers were linear ($Y = \alpha X + b$). The equations presented by Heidari et al. [44] had better determination coefficients than the Yılmaz and Yuksek's [38] equation.

Due to the little research done in the past on the correlation between UCS, APLI and DPLI in sulfate rocks, in this research, an attempt was made to perform UCTs and axial-diametral point load tests on these rocks and making a correlation between their test results, to investigate:

1. the reliability of two types of point load tests in predicting UCS,
2. obtains the conversion factors between the strength properties of sulfate rocks with different mineral compositions,
3. the effect of mineral composition on these correlations, and
4. the deformation behavior of loading points in point load tests during the experiments.

Table 1 Relationships presented by different researchers between UCS and $I_{s(50)}$ for different rocks

Author(s)	Suggested correlation equation	R^2	Rock
D'Andrea et al. [9]	UCS = 15.3 PLI + 16.3	-	Granite, basalt, rhyolite, serpentine, slate, sandstone, limestone, dolomite, taconite, syenite pegmatite, anorthosite, chalk, marble, schist, peridotite, quartzite, gabbro, greenstone
Deere and Miller [12]	UCS = 20.7 $I_{s(50)}$ + 29.6	-	limestone, granite, basalt
Broch and Franklin [3]	UCS = 23.7 $I_{s(50)}$	-	Various rock types
Bieniawski [5]	UCS = 23.9 $I_{s(50)}$	-	different rock type
Hassani et al [13]	UCS = 29 PLI	-	Sedimentary rocks
Read et al. [14]	UCS = 16 $I_{s(50)}$	-	Sedimentary rocks
	UCS = 20 $I_{s(50)}$	-	Basalt
Singh [15]	UCS = 18.7 $I_{s(50)}$ − 13.2	-	Sandstone, sandy shale, ferruginous sandstone etc.
Forster [8]	UCS = 14 $I_{s(50)}$	-	-
Gunsallus and Kulhawy [16]	UCS = 16.5 $I_{s(50)}$ + 51.0	-	Sandstone
ISRM [1]	UCS = (20, …, 25) $I_{s(50)}$	-	All rocks
Das [17]	UCS = 14.7 PLI	-	Siltstone
	UCS = 18 PLI	-	Sandstone
	UCS = 12.6 PLI	-	Shale
Hawkins and Olver [18]	UCS = 26.5 PLI	-	Limestone
	UCS = 24.8 PLI	-	Sandstone
O'Rourke [19]	UCS = 30 PLI	-	Sedimentary
Vallejo et al. [20]	UCS = 17.4 $I_{s(50)}$	-	Sandstone
	UCS = 12.6 $I_{s(50)}$	-	Shale
Cargill and Shakoor [21]	UCS = 23 $I_{s(50)}$ + 13	-	Sandstone, limestone
Tsidzi [22]	UCS = (14, …, 82) $I_{s(50)}$	-	Metamorphic rocks
Ghosh and Srivastava [23]	UCS = 16 $I_{s(50)}$	-	22 Granite rock samples
Grasso et al. [24]	UCS = 25.67 $(I_{s(50)})^{0.57}$	-	Power relation
	UCS = 9.30 $I_{s(50)}$ + 20.04	-	Linear relation
Singh and Singh [25]	UCS = 23.37 $I_{s(50)}$	0.80	Quartzite
Ulusay et al. [26]	UCS = 19 $I_{s(50)}$ +12.7	-	Sandstone
Chau and Wong [27]	UCS = 12.5 $I_{s(50)}$	0.73	Granite and tuff
Smith [28]	UCS = 24 $I_{s(50)}$ = 14.3 $I_{s(50)}$	-	Sandstone/limestone
	UCS = 12.6 PLI	-	Shale
Rusnak and Mark [29]	UCS = 21.8 PLI	-	Shale
	UCS = 20.2 PLI	-	Siltstone
	UCS = 20.6 PLI	-	Sandstone
	UCS = 21.9 PLI	-	Limestone
Tuğrul and Zarif [30]	UCS = 15.25 $I_{s(50)}$	0.98	Granite
Kahraman [31]	UCS = 8.41 $I_{s(50)}$ + 9.51	0.85	Dolomite, limestone
	UCS = 23.62 $I_{s(50)}$ − 2.69	-	Coal measure rocks
Sulukcu and Ulusay [32]	UCS = 15.31 $I_{s(50)}$	0.83	23 samples in different rock type
Quane and Russel [33]	UCS = 24.4 $I_{s(50)}$	-	Welded ignimbrite
	UCS = 3.86 $I_{s(50)}^{2}$ + 5.65 $I_{s(50)}$	-	Pyroclastic rocks
Tsiambaos and Sabatakakis [34]	UCS = 7.3 $I_{s(50)}^{1.71}$	-	Power relation (Limestone-Sand stone- Marlstone)
	UCS = 23 $I_{s(50)}$	-	Linear relation (Limestone-Sand stone- Marlstone)
Fener et al. [35]	UCS = 9.08 $I_{s(50)}$ + 39.32	0.85	Igneous - metamorphic - sedimentary rocks
Kahraman et al. [36]	UCS = 10.91 PLI + 27.41	-	Various rock types Porosity>1%
Agustawijaya [37]	UCS = 13.4 $I_{s(50)}$	0.89	Various rock types

Table 1 Relationships presented by different researchers between UCS and $I_{s(50)}$ for different rocks (continued)

Author(s)	Suggested correlation equation	R^2	Rock
Yılmaz and Yuksek [38]	UCS = 12.4 $I_{s(50)}$ – 9.0859	0.81	Gypsum
Diamantis et al. [39]	UCS = 19.79 $I_{s(50)}$	0.74	Serpentinite
Sabatakakis et al. [40]	UCS = 13 $I_{s(50)}$, I_s < 2 MPa	0.70	Marlstones
	UCS = 24 $I_{s(50)}$, I_s = 2–5 MPa	0.60	Sandstones
	UCS = 28 $I_{s(50)}$, I_s > 2 MPa	0.72	Limestones
Kahraman and Gunaydin [41]	UCS = 8.20 I_s + 36.43	0.68	Igneous rocks
	UCS = 18.45 I_s – 13.63	0.77	Metamorphic rocks
	UCS = 29.77 I_s – 51.49	0.78	Sedimentary rocks
Basu and Kamran [42]	UCS = 11.103 $I_{s(50)}$ – 37.66	-	Schistose rocks
Tahir et al. [43]	UCS = 21.69 $I_{s(50)}$	0.30	Limestone
Heidari et al. [44]	UCS = 5.58 $I_{s(50)}$ + 21.92	0.93	Gypsum; (axial) - Air dried
	UCS = 7.56 $I_{s(50)}$ + 23.68	0.94	Gypsum; (diametric) - Air dried
	UCS = 3.50 $I_{s(50)}$ + 24.84	0.89	Gypsum; (irregular) - Air dried
	UCS = 10.99 $I_{s(50)}$ + 7.04	0.92	Gypsum; (axial) - Saturated
	UCS = 11.96 $I_{s(50)}$ + 10.94	0.94	Gypsum; (diametric) - Saturated
	UCS = 13.29 $I_{s(50)}$ + 5.25	0.90	Gypsum; (irregular) - Saturated
Karaman and Kesimal [45]	UCS = 20.42 $I_{s(50)}$ − 5.146	-	Various rock types
Kohno and Maeda [46]	UCS = 16.4 $I_{s(50)}$	0.92	Various rock types
Basu [47]	UCS = 11.218 $I_{s(50)}$ + 4.008	-	Schistose rocks
Singh et al. [48]	UCS = 22.8 $I_{s(50)}$	0.99	Schist
	UCS = 21.9 $I_{s(50)}$	0.89	Sandstone
	UCS = 21 $I_{s(50)}$	0.96	Epidiorite
	UCS = 22.3 $I_{s(50)}$	0.68	Limestone
	UCS = 22.7 $I_{s(50)}$	0.82	Dolomite
Mishra and Basu [49]	UCS = 14.63 $I_{s(50)}$	0.99	Sandstone- Schist-Granite
Li and Wong [50]	UCS = 19.831 $I_{s(50)}$	-	Meta-siltstone
	UCS = 21.27 $I_{s(50)}$	-	Meta-sand stone
Tandon and Gupta [51]	UCS = 5.6 $I_{s(50)}$ + 4.38	0.94	Granite
	UCS = 8.597 $I_{s(50)}$ + 30.72	0.78	Quartzite
	UCS = 10.53 $I_{s(50)}$ − 7.61	0.91	Dolomite
Kahraman [52]	UCS = 14.68 $I_{s(50)}$ − 8.67	0.88	Pyroclastic rocks
Momeni et al. [53]	UCS = 13.54 $I_{s(50)}$ + 14.93	0.74	Limestone-Shale-Granite

The difference of this research with other similar researches is, firstly, the correlation between the results of the uniaxial compressive strength and axial and diagonal point load tests in a relatively wide range of mineral composition of sulfate rocks, secondly, for the first time, an attempt was made to investigate the correlations between the results of point load tests and the mineral composition of sulfate rocks, and for the first time, presents the deformation behavior of loading points in point load tests.

2 Geology setting

One of the most typical gypsum (GP) and anhydrite (AN) bearing formations in the middle east is the Gachsaran Formation (Southeast-Northwest of Iran in the Zagros zone, formerly Low Fars), which meets the North-West regions of Iraq. This formation consists of a sequence of marl, lime, gypsum, anhydrite layers and in some areas, salt layers. Therefore, this formation is susceptible to erosion, dissolution, physical and chemical degradation. The Gachsaran Formation comprises seven members. The first member (the lowest one), which is made up of AN, is known as the caprock of the Asmari carbonate reservoir, the most famous hydrocarbon reservoir in Iran [66]. One of the most important hydraulic structures that affected by the GP layers of the formation is the Mosul Dam in Iraq, which faced significant problems such as dissolving and karstification of the dam

foundation [67–70]. Based on macroscopic evidence (texture, color of the crystals and matrix), in 84 rock blocks collected from the 4 dam sites, 20 appearance types (Konjun-Cham dam site 4 types, Meymeh dam site 5 types, Kangir dam site 7 types, and Nargesi dam site 4 types) were identified. The lithological studies showed that, in general, the studied rocks consist of GP, AN, clay minerals (CMs) with the differential contribution of each of these minerals in the rock samples. So that the core samples were taken from the rock blocks collected from the Konjun-Cham dam site contain large crystals in a cream to light to dark earthy color matrix (porphyry texture), mainly of gypsy nature with a maximum content of about 31% of CMs, the samples of the Meymeh dam site have a dark gray to light earthy color and porphyry texture, with a higher content of AN along with CMs up to 12%, but generally, in microscopic studies, amorphous salt crystals can be found in the rock matrix, the samples of the Kangir dam site are gray to dark earthy color, with alabaster texture, mainly of gypsy nature, almost without AN, but with CMs up to 18%, and the samples of the Nargesi Dam site in gray color, with alabaster texture, mostly of gypsy nature, almost without AN, but some samples have CMs even up to 59%. The average porosity, dry and saturated density of GP rocks, was 1.87 ± 0.61%, 2.35 ± 0.12, 2.37 ± 0.13 g/cm^3 and AN rocks 2.13 ± 0.72%, 2.56 ± 0.11, 2.62 ± 0.07 g/cm^3, respectively. But it should be noted that the actual saturated density of these types of soluble rocks will be a little more than the measured values due to their surface dissolution during saturation.

In 2020, because more than 30 large reservoir dams were being understudied or under construction within or adjacent to the Gachsaran problematic Formation in Iran, and importance of the identifying engineering and strength properties of the GP and AN layers of this formation, this research was carried out on sulfate rock blocks taken from the outcrops of this evaporative formation at Konjun-Cham, Meymeh, Nargesi, and Tange-Shemiran (the other name, Kanghir) under construction dam sites. In Fig. 1 [71], the geographic location of the studied dam sites is shown on the geographical map of Iran.

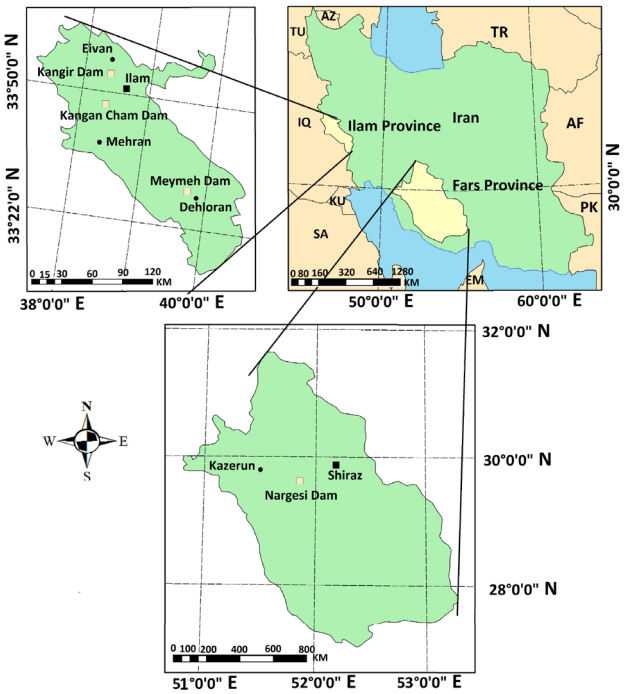

Fig. 1 Geographic location of studied dam sites on a geographical map of Iran National Cartographic Center (with modifications) [71]

3 Materials and methods

3.1 Sampling and preparation of samples

The rock blocks used in this research with dimensions about 40 × 30 × 30 cm, were collected from the exposed sulfate rock layers of the Gachsaran Formation from the Konjun-Cham (16 blocks), Meymeh (35 blocks), Nargesi (17 blocks), and Kangir (16 blocks) reservoir dam sites in Iran (totally, 84 rock blocks). Also, seven rock blocks were gathered from the exposed Aghajari Formation downstream of the Konjun-Cham dam axis to investigate the effect of CMs on gypsum properties. In this paper KG, MG, NG and TG indexes were used for rock blocks gathered from the outcrops of the Gachsaran Formation at the Konjun-Cham, Meymeh, Nargesi and Kangir dam sites and KA for rock blocks belong to the Aghajari Formation, respectively. After transferring the rock blocks to the Geological and Geotechnical Laboratory of Bu-Ali Sina University, coring with dimensions of *NX* (54.7 mm) was performed. For UCT samples, the *L*/*D* ratio was selected close to 1:2.5 to meet the dimensional specifications of core samples specified in both ASTM D7012-23 [72] and ISRM [73] standards. The two ends of the samples were polished completely, and flawless samples were used in experiments. A steel platform and two wagon rails installed on the platform were used in two directions perpendicular to each other to ensure that the sample dimension tolerances meet ASTM D4543-19 [74] standard. By installing the gauge on the wagons and moving the gauge needle on the body of the sample and the two ends of the samples, the compliance of the sample's specifications with the standard criteria was checked. If the sample does not meet the standards, they were modified or removed. Fig. 2 shows several cylindrical rock core samples prepared from rock blocks taken from

Fig. 2 Rows of red, yellow, green and black, respectively, several rock core samples of the Konjun-Cham, Meymeh, Kangir and Nargesi dam sites

the four mentioned above dam sites for UCTs. Axial point load tests (APLTs) and diametral point load tests (DPLTs) samples were prepared from rock cores of approximately *NX* diameter by diamond cutting blade perpendicular to the longitudinal axis direction of the cores in accordance with the dimensional requirements specified in ISRM [1] and ASTM D5731-16 [2]. The length-to-diameter ratio of APLT specimens about 1/3 to 1, and the DPLT specimens larger than 1 (to 1.2) were selected. The specimens were prepared so that the two side circular surfaces of the specimens were completely parallel to each other. The diameter and length of all samples were determined using a digital caliper with an accuracy of 0.01. The diameter was measured in two perpendicular directions from the cylindrical surface, and the length was measured in two perpendicular directions on both lateral surfaces of the rock cores (4 measurements in total). The methods mentioned in Section 3.3 were used for oven-dried or saturate the samples.

3.2 Petrology

For the petrology of rock blocks, three methods were used, including microscopic studies (thin sections), X-ray diffraction (XRD) and X-ray fluorescence spectroscopy (XRF). In microscopic studies, first minerals were identified and then an image analysis method was used to determine the volume content of minerals. For this purpose, Adobe Photoshop software was used. The microscopic studies indicate that the main constituent minerals of samples include GP ($CaSO4 \bullet 2H_2O$), AN ($CaSO_4$) (Fig. 3 (b)), and CMs [75]. The predominant texture of the Nargesi and Kangir dam sites rock samples was alabaster (microcrystalline) (Fig. 3 (a)), and Konjun-Cham and Meymeh dam sites were found in the porphyry texture (Fig. 3 (c)). The rock blocks gathered from the Aghajari Formation had alabaster texture in one sampling location and porphyry texture in another location. One of the important issues observed in microscopic studies is the presence of clay-sized carbonated minerals (microcrystalline carbonates) inside or along with clay minerals (Fig. 3 (a)), so the clay minerals found in investigated samples can be identified as carbonated clay minerals. X-Powder software was used to analyze the XRD diffractograms. The RIR (Reference Intensity Ratios) quantitative analysis method was also used to quantify the minerals. In some samples, the GP mineral is dominant, and in some cases, the amount of AN is higher. The minor minerals include calcite, dolomite, quartz, CMs (such as Illite, Kaolinite, Montmorillonite, Chlorite), and some kinds of Halite (including Halite, Cryptohalite, Sinhalite, Sulphohalite, Hydrohalite, Polyhalite). In XRD studies, it has been possible to identify the kind of CMs and detect some other minerals, such as halite, which are usually not detectable in microscopic studies (Table 2). These studies indicate that in some regions the Gachsaran Formation contains halite minerals. The presence of halite

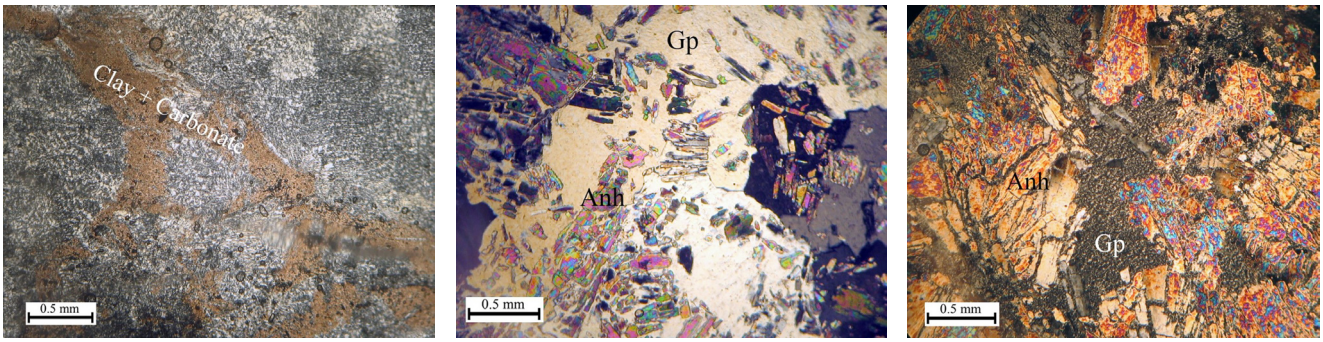

(a) (b) (c)

Fig. 3 Microscopic thin sections image of (a) an alabaster gypsum, (b) a gypsum dominant, (c) an anhydride dominant rock

Table 2 XRD analysis results

Rock group	Gypsum	Anhydrite	Calcite	Dolomite	Halite	Quartz	Illite	Kaolinite	Montmorillonite	Chlorite	Amorf
KA1-2	89.4	4.1	0	0	0	2.1	0	2.1	0	0	2.3
KA2-1	58.3	5.5	0	0	0	0	10.5	6.6	0	15.8	3.2
KG1-1	52.5	2.15	24.8	0	1.85	1.6	3.1	2.65	2.1	5.6	3.15
KG2-1	55.4	2	18.4	0	0	0.8	1.8	12.1	3.4	1.8	4.1
KG3-1	2.7	93.5	1.9	0	0	0	0	1.9	0	0	0
KG4-1	29.05	40	8.75	1.45	0	2.25	5.1	2.55	2.1	2.1	6.65
MG1-2	53.6	1.5	10.5	0	0	2.6	6.9	9.3	6.8	4.7	4.3
MG2-2	6.5	77.8	4.4	4.4	0	0	1.4	0	1.2	0	4.3
MG3-1	16.8	72.8	0	0	0	0.7	3.6	1	0	0.8	4.3
MG4-2	14.1	59.1	6.4	5	0	0.5	5.8	2.5	0	1.8	4.6
MG4-5	14	66.7	5	3	0	0.9	0.5	1.9	1.4	2.1	4.6
NG1-1	73.8	0	13.3	7.1	3.3	0	0	0.4	0	0	2.1
NG2-1	87.7	0	0	0	0	3.6	0	0	8.7	0	0
NG2-2	60.2	0.4	0	19.8	0	2.4	1.3	2.3	1.2	6	6.3
TG1-1	96.4	0	0	0	0	0	0	1.5	0	0	2.1
TG2-1	93.4	0	0	0	0	3.4	0	0	0	0	3.2

minerals in the Gachsaran Formation can be the source of salt deposits observed on the margins of some rivers. Carbonate minerals (calcite and dolomite) were even up to 25% observed in XRD results. The results of the XRF analysis confirmed that the main constituent oxides of the samples are the main constituent oxides of GP and AN. In XRF results, on average, 36% and 46%, CaO and SO_3 were observed in the tested specimens, respectively (Table 3). These two oxides, with such percentages, actually reflect the sulfate nature of the studied rocks. Also, the presence of aluminum, magnesium, iron and silica oxides indicates the presence of CMs in the samples.

3.3 Drying and saturating of samples

Owing to low permeability ($x \times 10^{-7}$ to $x \times 10^{-9}$ cm/s) and sulfate rocks' dissolving and swelling properties, preparing these rocks to perform UCT and PLT in dry and saturated conditions encounters some problems. Although microwave oven heating has been proposed by standard test method [72] for the determination of water content of soil samples during the last few decades, in order to dry rock samples, the oven has been adopted in place of the microwave. Regarding the sample sensitivity issue in the current study, an attempt was made to use a different method for thoroughly drying and saturating the sulfate

Table 3 XRF analysis results

Rock group	SiO_2 (%)	Al_2O_3 (%)	CaO (%)	MgO (%)	TiO_2 (%)	Fe_2O_3 (%)	SO_3 (%)	P_2O_5 (%)	Na_2O (%)	K_2O (%)	SrO (%)	ZrO_2 (%)	L.O.I (%)
KG1-1	2.07	0.63	31.25	1.15	<0.1	0.53	42.34	<0.1	<0.1	<0.1	0.13	<0.1	21.92
KG2-1	0.88	0.24	36.47	<0.1	<0.1	<0.1	39.51	<0.1	<0.1	<0.1	0.18	<0.1	22.73
KG3-1	0.21	0.06	38.87	<0.1	<0.1	<0.1	52.45	<0.1	<0.1	<0.1	0.17	<0.1	8.24
KG4-1	0.81	0.23	37.66	<0.1	<0.1	<0.1	52.65	<0.1	<0.1	<0.1	0.19	<0.1	8.45
MG2-2	<0.1	<0.1	39.78	<0.1	<0.1	<0.1	53.6	<0.1	<0.1	<0.1	0.21	<0.1	6.41
MG3-1	0.83	0.25	32.68	0.57	<0.1	<0.1	43.37	<0.1	<0.1	<0.1	0.87	0.18	21.25
MG4-2	0.61	0.16	38.24	<0.1	<0.1	<0.1	52.15	<0.1	<0.1	<0.1	0.45	0.08	8.31
NG2-2	0.55	0.21	34.32	<0.1	<0.1	<0.1	43.42	<0.1	<0.1	<0.1	0.85	0.16	20.49
TG1-1	0.63	0.17	34.31	0.45	<0.1	<0.1	42.74	<0.1	<0.1	<0.1	0.33	<0.1	21.36
TG2-1	2.78	0.83	31.52	0.71	<0.1	<0.1	41.05	<0.1	<0.1	0.34	0.45	0.1	22.22
Sum			355.1				463.3						161.4
Mean			35.51				46.33						16.14

rock samples. The result of this study showed that with a temperature of 45 ± 2 °C for drying sulfate rock samples (to prevent GP dehydrating and turning into AN), the usual multi-day time used in geotechnical labs is not enough time. Moreover, achieving a constant or near-constant weight of GP samples needs at least 2 to 4 weeks [76]. This time for the AN samples lasts more than a year sometimes. In this research, by giving such time opportunities to the samples, it was attempted to dry the samples completely with losing free water. Additionally, vacuum pressure method by using a desiccator and a suction pump was used for saturating samples. The performed experiments confirmed that, generally, the samples subjected to a wet vacuum pressure of $P_{vac(\text{wet})} = -0.5$ atmosphere (atm) for four days, gaining more than 95 % of their added weight, and practically the sample could be considered saturated. Before applying the wet vacuum pressure, a dry vacuum pressure ($P_{vac(\text{dry})}$) stage was applied to the samples to create an internal negative pressure inside the samples, for more and faster water absorption during the wet vacuum pressure. In the case of GP - AN rocks, the experiences showed that the application of a dry vacuum pressure equivalent to −0.5 atm for five hours ($P_{vac(\text{dry})} = -0.5$ atm, $T_{vac(\text{dry})} = 5$ h) gives beneficial results [77].

3.4 Test procedures

To perform a dry UCS test, after drying the core sample in the oven, first, the sample was cooled inside the desiccator, and its temperature was balanced to ambient temperature, and then it was subjected to UCT. UCTs were performed using a uniaxial compression testing device ELE international 2000 model, load gauge with an accuracy of 0.01 kN (Newton), strain gauge with an accuracy of 0.001 mm, a data logger and a computer for viewing and recording data. The UCTs were performed according to ASTM D7012-23 [72] and ISRM [73] standards. Saturated core samples were tested in the same way as dry samples after removing them from water and drying their surface with a cotton cloth. The average loading rate was selected about 200 N/s to meet the failure time criteria specified in the standard ISRM [73] (5 to 10 minutes) and ASTM D7012-23 [72] (2 to 15 minutes), at an appropriate time of about 5 to 15 minutes, as well as they can enter the failure stage without entering the creeping stage [78]. Loading continued on each sample until failure occurred. The longitudinal strain of the sample was measured using a strain gauge. Point load tests were performed by using the UCT mentioned device. By installing steel conical platens on the mentioned device's upper and lower steel plate surfaces and placing the sample between the tips of the two conical platens, the load was applied at a constant rate until the rupture occurred in the sample. The experiments were performed by Broch and Franklin [3], ISRM [1] and ASTM D5731-16 [2]. The loading rates were chosen to break the samples at the specified time of 10 to 60 seconds in the two mentioned standards. Experience has shown that about 0.1 KN/sec is the appropriate rate for such experiments in sulfate rocks. According to paragraphs 8–5 of ASTM D5731-16 [2], if the amount of penetration of conical platens into the sample is significant, D' (distance between the tips of two conical platens at the time of sample rupture) should be used instead of the initial D (Initial sample thickness) value of the sample. Therefore, due to the significant penetration of the conical planets into the tested rock samples in this research, the amount of penetration into the two end surfaces of the APLT specimens and also the two sides of the diameter of the DPLT specimens were measured by installing a strain gauge on the lower metal platen of the UCT device during the experiments.

3.5 Calculations

To calculate the UCS of each specimen, the failure load (F in kN), the original cross-section area (A in m^2) of the sample and equation UCS = F/A were used (according to ASTM D7012-23 [72] and ISRM [73]). To estimate the PLI or I_s according to ISRM [1] and ASTM D5731-16 [2], the uncorrected PLI was calculated using $I_s = P/De^2$ equation. In this equation, P = failure load (N), De = equivalent core diameter = D for diametral tests (m) given by $De^2 = D^2$ for cores (mm^2) or $De^2 = 4A/\pi$ for axial, block, and lump tests (mm^2), where $A = WD$ = minimum cross-sectional area of a plane passing through the platen contact points. The modified De values are calculated as follows:

$$De^2 = D \times D' \text{for cores} = 4/\pi\, W \times D' \text{for other shapes.} \quad (3)$$

Because in this research, cores of about NX were used in the experiments, to verify the results and better compare the results with other similar studies, size correction was made in the test results. Size correction is done using the $I_{s(50)} = F \times I_s$ equation. The size correction factor F is calculated from the $F = (De/50)^{0.45}$ equation. Therefore, by calculating the size correction factor and applying it to the unmodified PLI, the result of the PLT of each sample is modified to a sample equivalent to a 50 mm core sample and $I_{s(50)}$ is calculated. To estimate the mean $I_{s(50)}$, depend on the number of samples of each groups kind of rocks,

according to ISRM [1] and ASTM D5731-16 [2], the two highest and two lowest values from the ten or more valid tests was removed and the rest was averaged. In the case of rock samples with less than 10 experiments, a maximum and minimum values was removed.

4 Results

In this study, the results of 182 series of laboratory tests (182 UCTs, 182 APLTs and 182 DPLTs in dry and saturated conditions, a total of 1092 tests) were used. The results of the experiments performed on the oven-dried samples are presented in Appendix A and saturated conditions in Appendix B. In the coding of each sample, the first two letters are the abbreviation of the sampled dam site (KG for the Kunjan-cham dam, MG for the Meymeh dam, TG for the Kangir dam and NG for the Nargesi dam), the first number after the first two letters, the sampling location number, the second and the third number is the rock block number and the UCT sample number. The mean length (L), diameter (D), L/D ratio of UCT specimens is 133 ± 3.40, 53.53 ± 0.86 mm and 2.49 ± 0.07, respectively. The mean L, D, L/D ratio of APLT specimens is 26.34 ± 1.90, 53.39 ± 1.11 mm and 0.49 ± 0.30 and DPLT specimens were 58.77 ± 1.35, 53.75 ± 0.47 mm and 1.09 ± 0.03, respectively.

Table 4 Mineralogical classification of the rock samples at each sampling site

Row	Dam site	Rock group	Mineral composition%			Texture
			GP	AN	CMs	
1	Konjun-Cham	KA1-2	68.89	1.70	29.41	Alabaster
2		KA2-1	87.31	2.32	10.37	Porphyry
3		KG1-1	91.31	1.60	7.10	Porphyry
4		KG2-1	70.38	0.38	29.23	Porphyry
5		KG3-1	20.27	75.27	4.46	Porphyry
6		KG4-1	50.19	26.72	23.09	Porphyry
7	Meymeh	MG1-2	59.37	38.98	1.69	Porphyry
8		MG2-1	86.37	10.76	2.86	Porphyry
9		MG2-2	23.94	71.44	4.63	Porphyry
10		MG3-1	18.73	81.27	0.00	Porphyry
11		MG4-2	49.22	50.18	0.60	Porphyry
12		MG4-5	29.07	69.16	1.77	Porphyry
13	Nargesi	NG1-1	75.70	9.00	15.29	Alabaster
14		NG2-1	89.49	0.61	9.89	Alabaster
15		NG2-2	43.90	46.53	9.57	Alabaster
16	Kangir	TG1-1	93.04	1.33	5.62	Alabaster
17		TG2-1	93.92	1.52	4.65	Alabaster
Mean			61.83	28.75	9.43	
Max			93.92	81.27	29.41	
Min			18.73	0.38	0.00	
St.D			27.30	30.85	9.46	

5 Discussions

Regression analysis between the APLTs - DPLTs results with the results of UCTs experiments in dry and saturated conditions was performed in two ways: analysis of the results of experiments of rock groups with specific mineral composition (samples with almost identical mineral composition taken from the rock blocks belong to a specific sampling site) and the results of all tested samples with their general classification in the form of three main mineral composition groups (samples with almost identical mineral composition taken from rock blocks gathered from the different sampling site).

5.1 Analysis based on the mineral composition of rock groups

In this type of analysis, the results of 182 UCTs, 182 APLTs and 182 DPLTs in dry conditions (182 series) and with the same number in saturated conditions were used. The grouping of the samples related to each specific sampling site based on the mineral composition, led to the placement of the samples in 17 rock groups (Table 4), including 4, 6, 3 and 2 rock groups belonging to the rock blocks gathered from the Gachsaran Formation outcrops in sampling sites in the Konjun-cham, Meymeh, Kangir and Nargesi dam sites, respectively and also, two rock groups contain samples of rock blocks taken from the Aghajari Formation outcrops (rock groups KA1-2 and KA2-1). In this method, regression analysis of n triples of the results of APLTs-DPLTs and UCTs of each rock group was performed. The value of n varied from a minimum of 8 to a maximum of 15.

Fig. 4 shows several tested samples from many rock groups with valid results before and after APLT Experiments. In the results of valid experiments, the failure surface clearly passed through both loading points, and the specimens are broken approximately in the direction perpendicular to the axis of the specimens, and the specimens are divided into two to three separate pieces. In DPLTs specimens, in valid failure (Fig. 5) the failure surface generally passes through both loading points as a surface approximately perpendicular to the axis of the specimen. But in a limited number of samples, the failure surface also occurs in the diametral direction. Following

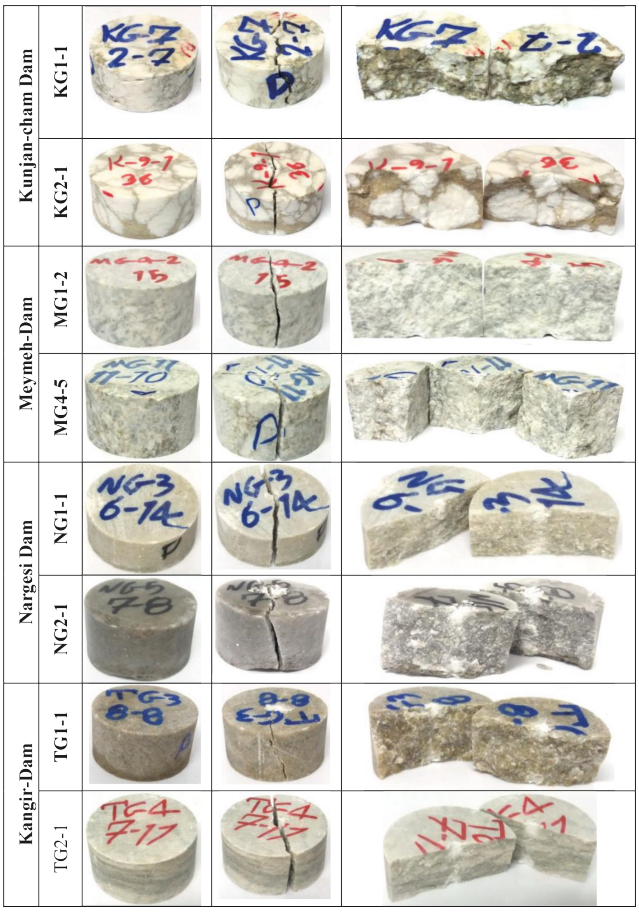

Fig. 4 Examples of valid axial point load tests results of rock groups (this study)

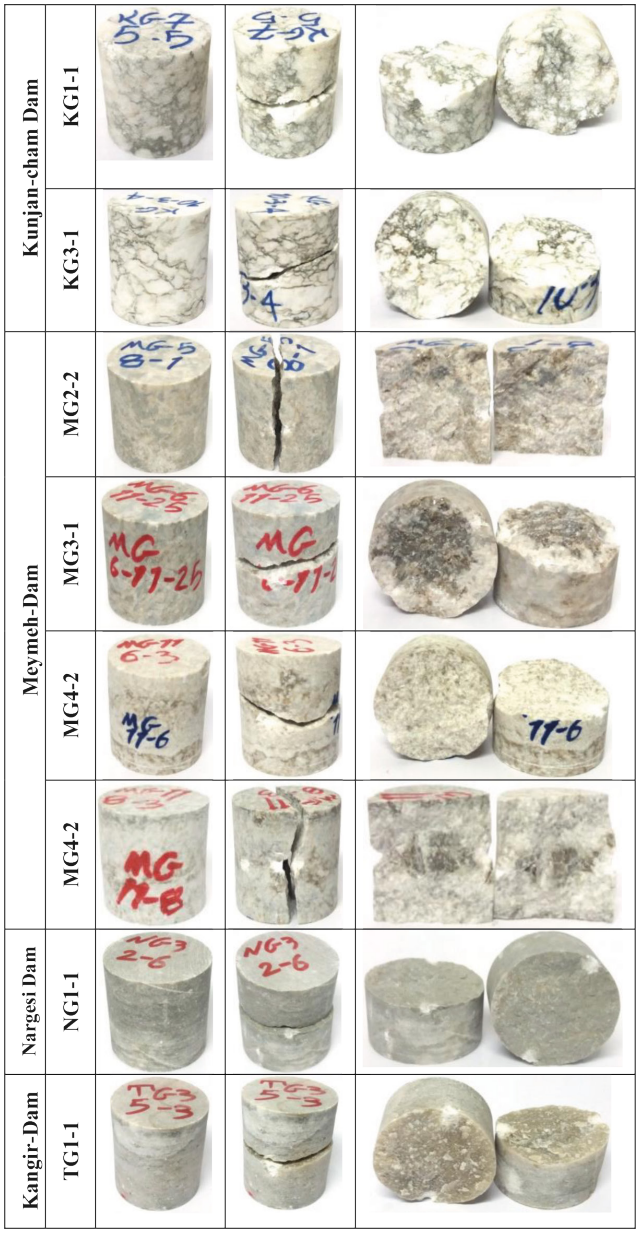

Fig. 5 Examples of valid diametral point load tests results of rock groups (this study)

the ASTM D5731-16 [2] and ISRM [1] standards, the use of the results of samples with invalid failure was avoided in the analysis.

Fig. 6 shows examples of invalid APLTs (Fig. 6 (a)) and DPLTs (Fig. 6 (b)) results experienced in this study. As can be seen in these samples, the failure could not pass through both or one or neither loading points.

The best-fitted curves on the data points (e.g., Fig. 7) were extracted, and their equations were obtained by regression analysis on each rock group experiment result in both dry and saturated conditions. Given that the predominant equation type in the reported global equations so far (Table 1) is basically the first-degree equation (UCS = $\alpha\ I_{s(50)} \pm b$), so if the determination coefficients (R^2) for the best-fitted equations are of the exponential, logarithmic or power type and had a maximum difference of 2% with linear equations, first-order equations were selected for easier comparison with common linear equations. In Table 5, the axial equations are presented for the correlation between UCS and $I_{s(50)(\text{Axial})}$ and the diametral equations for the correlation between UCS and $I_{s(50)(\text{Diametral})}$ for the 17 rock groups in dry and saturated conditions. In Table 5, except for one case (the axial equation in row 6 in the dry condition part), all the extracted equations are linear, and secondly, the mean determination coefficients for both UCS − $I_{s(50)(\text{Axial})}$ and UCS − $I_{s(50)(\text{Diametral})}$ correlations are greater than 0.90, therefore, the extracted equations have perfect predictability for UCS in dry and saturated conditions. The relationships obtained in this study for almost pure gypsum rock groups (KG1-1, TG1-1 and TG2-1 rock groups in Table 5) are similar to report by Yılmaz and Yuksek [38] and Heidari et al. [44], but with different coefficients for the X variable (α values) and different y-intercept values

(a)

(b)

Fig. 6 Examples of invalid test results in (a) APLTs and (b) DPLTs (this study)

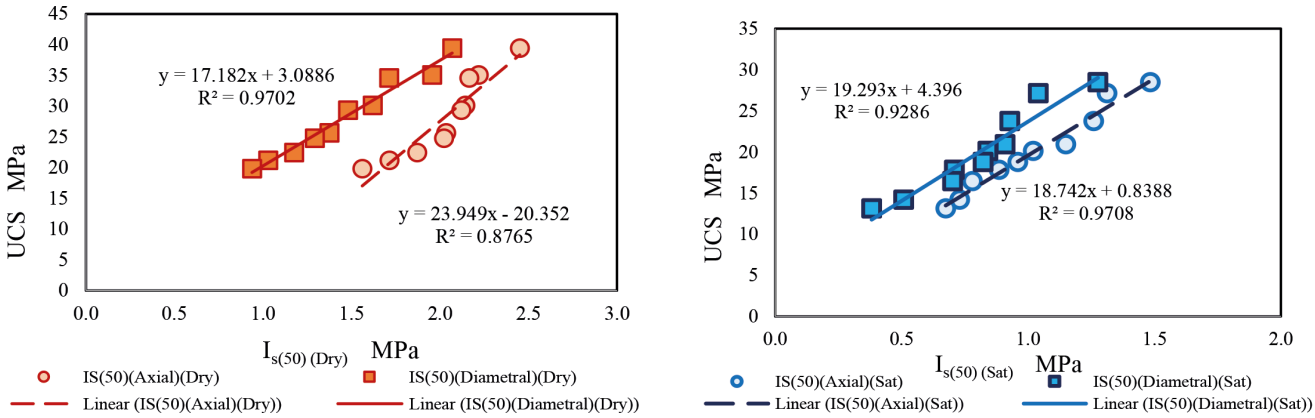

(a) (b)

Fig. 7 The correlation between UCS and $I_{s(50)(\text{Axial})(\text{Dry})} - I_{s(50)(\text{Diametral})(\text{Dry})}$ for the NG1-1 rock group in (a) Dry conditions, (b) Saturated conditions

(*b* values) in equations. Any researcher can use the equations presented in Table 5 to compare their similar research results on sulfate rocks (with a similar mineral composition to each rock group). To estimate the average APLI and DPLI of each rock group, in accordance with paragraph 10.3.2 of ASTM D5731-16 [2] and paragraph 14 (b) of the ISRM [1], first the maximum and minimum values of $I_{s(50)(\text{Axial})}$ or $I_{s(50)(\text{Diametral})}$ were removed (depending on the number of performed experiments, one to two values of maximum or minimum) and then the average value was calculated from the remaining number of $I_{s(50)}$. In addition to applying these rules to the results of APLTs and DPLTs, to create homogeneity, the same procedure was used for the results of UCTs. In Table 6, the values of APLI - DPLI and UCSs calculated for each rock group are presented in dry and saturated conditions. In Table 6, the KG1-1 (porphyry),

Table 5 Extracted correlation equations between UCS and $I_{s(50)(Axial)(Dry)} - I_{s(50)(Diametral)(Sat)}$ for each rock group in dry and saturated conditions

Row	Rock group	Number of sample	$I_{s(50)(Axial)}$ Equation	R^2	$I_{s(50)(Diametral)}$ Equation	R^2
			Dry condition			
1	KA1-2	15	UCS = 9.34 $I_{s(50)(Axial)(Dry)}$ + 12.07	0.80	UCS = 9.88 $I_{s(50)(Diametral)(Dry)}$ + 11.49	0.96
2	KA2-1	10	UCS = 11.98 $I_{s(50)(Axial)(Dry)}$ + 11.28	0.94	UCS = 9.74 $I_{s(50)(Diametral)(Dry)}$ + 11.09	0.96
3	KG1-1	13	UCS = 10.13 $I_{s(50)(Axial)(Dry)}$ + 8.44	0.88	UCS = 6.50 $I_{s(50)(Diametral)(Dry)}$ + 12.41	0.90
4	KG2-1	9	UCS = 24.48 $I_{s(50)(Axial)(Dry)}$ − 19.68	0.90	UCS = 9.88 $I_{s(50)(Diametral)(Dry)}$ + 14.70	0.98
5	KG3-1	13	UCS = 16.25 $I_{s(50)(Axial)(Dry)}$ − 7.40	0.93	UCS = 15.56 $I_{s(50)(Diametral)(Dry)}$ − 1.74	0.98
6	KG4-1	11	UCS = 14.18 $I_{s(50)(Axial)(Dry)}$ 1.40	0.83	UCS = 13.58 $I_{s(50)(Diametral)(Dry)}$ + 9.49	0.94
7	MG1-2	8	UCS = 15.41 $I_{s(50)(Axial)(Dry)}$ + 8.52	0.96	UCS = 22.71 $I_{s(50)(Diametral)(Dry)}$ + 2.77	0.92
8	MG2-1	7	UCS = 10.43 $I_{s(50)(Axial)(Dry)}$ + 0.26	0.96	UCS = 7.30 $I_{s(50)(Diametral)(Dry)}$ + 7.42	0.94
9	MG2-2	12	UCS = 20.12 $I_{s(50)(Axial)(Dry)}$ − 11.24	0.94	UCS = 14.10 $I_{s(50)(Diametral)(Dry)}$ − 6.66	0.96
10	MG3-1	12	UCS = 15.20 $I_{s(50)(Axial)(Dry)}$ − 10.75	0.95	UCS = 14.49 $I_{s(50)(Diametral)(Dry)}$ − 5.94	0.95
11	MG4-2	10	UCS = 20.36 $I_{s(50)(Axial)(Dry)}$ − 2.78	0.96	UCS = 14.18 $I_{s(50)(Diametral)(Dry)}$ + 8.14	0.98
12	MG4-5	8	UCS = 17.45 $I_{s(50)(Axial)(Dry)}$ − 4.04	0.91	UCS = 11.00 $I_{s(50)(Diametral)(Dry)}$ + 13.18	0.87
13	NG1-1	10	UCS = 23.95 $I_{s(50)(Axial)(Dry)}$ − 20.35	0.88	UCS = 17.18 $I_{s(50)(Diametral)(Dry)}$ + 3.09	0.97
14	NG2.1	10	UCS = 12.91 $I_{s(50)(Axial)(Dry)}$ − 1.25	0.81	UCS = 12.33 $I_{s(50)(Diametral)(Dry)}$ + 3.74	0.96
15	NG2-2	8	UCS = 7.87 $I_{s(50)(Axial)(Dry)}$ + 9.30	0.99	UCS = 9.75 $I_{s(50)(Diametral)(Dry)}$ + 5.41	0.97
16	TG1-1	14	UCS = 16.88 $I_{s(50)(Axial)(Dry)}$ − 5.12	0.97	UCS = 16.64 $I_{s(50)(Diametral)(Dry)}$ − 6.61	0.96
17	TG2-1	12	UCS = 19.93 $I_{s(50)(Axial)(Dry)}$ − 10.59	0.93	UCS = 25.00 $I_{s(50)(Diametral)(Dry)}$ − 10.12	0.96
Mean				0.91		0.95
			Sat condition			
1	KA1-2	15	UCS = 31.60 $I_{s(50)(Axial)(Sat)}$ − 8.24	0.89	UCS = 34.23 $I_{s(50)(Diametral)(Sat)}$ − 7.34	0.87
2	KA2-1	10	UCS = 26.32 $I_{s(50)(Axial)(Sat)}$ − 1.50	0.94	UCS = 8.58 $I_{s(50)(Diametral)(Sat)}$ + 1.88	0.91
3	KG1-1	13	UCS = 20.94 $I_{s(50)(Axial)(Sat)}$ − 6.24	0.94	UCS = 10.47 $I_{s(50)(Diametral)(Sat)}$ − 0.08	0.94
4	KG2-1	9	UCS = 30.17 $I_{s(50)(Axial)(Sat)}$ − 2.64	0.95	UCS = 18.32 $I_{s(50)(Diametral)(Sat)}$ + 0.74	0.94
5	KG3-1	13	UCS = 25.49 $I_{s(50)(Axial)(Sat)}$ − 18.07	0.96	UCS = 16.18 $I_{s(50)(Diametral)(Sat)}$ − 3.17	0.98
6	KG4-1	11	UCS = 5.45 $I_{s(50)(Axial)(Sat)}$ + 14.31	0.94	UCS = 8.62 $I_{s(50)(Diametral)(Sat)}$ + 7.74	0.94
7	MG1-2	8	UCS = 18.75 $I_{s(50)(Axial)(Sat)}$ − 0.34	0.95	UCS = 18.18 $I_{s(50)(Diametral)(Sat)}$ + 11.57	0.98
8	MG2-1	7	UCS = 5.22 $I_{s(50)(Axial)(Sat)}$ + 15.24	0.75	UCS = 6.28 $I_{s(50)(Diametral)(Sat)}$ + 12.09	0.93
9	MG2-2	12	UCS = 12.99 $I_{s(50)(Axial)(Sat)}$ + 1.89	0.84	UCS = 5.94 $I_{s(50)(Diametral)(Sat)}$ + 10.38	0.88
10	MG3-1	12	UCS = 16.36 $I_{s(50)(Axial)(Sat)}$ − 4.88	0.98	UCS = 13.28 $I_{s(50)(Diametral)(Sat)}$ − 3.16	0.98
11	MG4-2	10	UCS = 17.17 $I_{s(50)(Axial)(Sat)}$ + 13.51	0.95	UCS = 12.55 $I_{s(50)(Diametral)(Sat)}$ + 14.19	0.96
12	MG4-5	8	UCS = 18.36 $I_{s(50)(Axial)(Sat)}$ − 4.49	0.94	UCS = 17.84 $I_{s(50)(Diametral)(Sat)}$ + 0.05	0.90
13	NG1-1	10	UCS = 18.74 $I_{s(50)(Axial)(Sat)}$ + 0.84	0.97	UCS = 19.29 $I_{s(50)(Diametral)(Sat)}$ + 4.40	0.93
14	NG2.1	10	UCS = 13.63 $I_{s(50)(Axial)(Sat)}$ + 2.13	0.96	UCS = 17.44 $I_{s(50)(Diametral)(Sat)}$ + 0.41	0.97
15	NG2-2	8	UCS = 5.52 $I_{s(50)(Axial)(Sat)}$ + 10.20	0.94	UCS = 6.09 $I_{s(50)(Diametral)(Sat)}$ + 10.61	0.91
16	TG1-1	14	UCS = 15.26 $I_{s(50)(Axial)(Sat)}$ + 3.66	0.95	UCS = 8.33 $I_{s(50)(Diametral)(Sat)}$ + 6.23	0.82
17	TG2-1	12	UCS = 13.86 $I_{s(50)(Axial)(Sat)}$ + 4.08	0.97	UCS = 22.97 $I_{s(50)(Diametral)(Sat)}$ + 2.49	0.81
Mean				0.93		0.92

TG1-1 (alabaster) and TG2-1 (alabaster) rock groups with more than 90% GP can be considered as almost pure gypsum rock groups (APGPRG), KG3-1, MG3-1, MG4-5 and MG2-2 (all with porphyry texture) with more than 69% AN as the anhydride dominant sulfate rock groups (ANDSRG), as well as KA1-2 and KG2-1 (both have porphyry texture) with about 29% of clay minerals, be considered as clay mineral bearing gypsum rock groups (CBGPRG). The mean UCS, $I_{s(50)(Axial)}$ and $I_{s(50)(Diametral)}$ of APGPRG samples in dry conditions are 23.75 ± 1.74, 1.74 ± 0.08 and 1.62 ± 0.47 MPa, respectively, and in saturated conditions, 13.36 ± 3.25, 0.77 ± 0.09 and 0.81 ± 0.17 MPa (Table 7).

Table 6 Mean UCS, $I_{s(50)(Axial)}$ and $I_{s(50)(Diametral)}$ of 17 sulfate rocks groups

Row	Sample NO	ρ			UCS			$I_{s(50)(Axial)}$			$I_{s(50)(Diametral)}$		
		Dry	Sat	Δ%	Dry	Sat	Δ%	Dry	Sat	Δ%	Dry	Sat	Δ%
1	KA1-2	2.21	2.22	0.45	27.30	21.46	−21.38	1.75	0.97	−44.51	1.64	0.87	−46.81
2	KA2-1	2.31	2.36	2.51	18.37	6.85	−62.68	0.62	0.33	−46.71	0.76	0.54	−29.19
3	KG1-1	2.08	2.28	9.71	25.72	9.65	−62.48	1.81	0.74	−58.94	2.16	0.88	−59.22
4	KG2-1	2.27	2.28	0.53	34.73	20.51	−40.95	2.25	0.77	−65.58	2.01	1.06	−47.49
5	KG3-1	2.64	2.70	2.19	33.47	31.62	−5.52	2.54	1.96	−23.01	2.22	2.15	−3.17
6	KG4-1	2.38	2.45	2.93	36.84	20.13	−45.35	2.08	1.03	−50.62	2.13	1.51	−28.90
7	MG1-2	2.60	2.69	3.49	57.28	50.86	−11.21	3.13	2.70	−13.96	2.36	2.16	−8.74
8	MG2-1	2.22	2.41	8.24	22.48	20.20	−10.17	2.12	0.90	−57.44	2.04	1.28	−37.41
9	MG2-2	2.54	2.59	2.09	34.47	24.88	−27.83	2.33	1.84	−21.02	3.01	2.54	−15.40
10	MG3-1	2.62	2.66	1.35	33.10	30.71	−7.22	2.88	2.18	−24.21	2.72	2.58	−4.91
11	MG4-2	2.67	2.72	1.94	54.57	51.72	−5.22	2.90	2.29	−21.25	3.36	2.99	−10.87
12	MG4-5	2.67	2.69	0.49	52.04	46.35	−10.94	3.24	2.81	−13.21	3.51	2.68	−23.80
13	NG1-1	2.28	2.32	1.51	27.83	19.62	−29.49	2.06	1.01	−50.98	1.44	0.82	−43.27
14	NG2-1	2.28	2.31	1.39	23.31	15.59	−33.11	1.92	1.01	−47.03	1.56	0.85	−45.15
15	NG2-2	2.28	2.31	1.43	22.06	18.04	−18.24	1.63	1.47	−10.20	1.73	1.28	−26.10
16	TG1-1	2.27	2.29	0.91	22.42	14.72	−34.37	1.66	0.71	−57.51	1.37	0.93	−32.12
17	TG2-1	2.26	2.29	1.37	23.11	15.70	−32.07	1.75	0.87	−50.29	1.34	0.62	−54.20
Mean		2.39	2.45	2.50	32.30	24.62	−26.95	2.16	1.39	−38.62	2.08	1.51	−30.40
St.D		0.19	0.18	2.59	11.96	13.50	18.40	0.65	0.76	18.67	0.74	0.82	17.55

Table 7 Mean UCS, $I_{s(50)(Axial)}$ and $I_{s(50)(Diametral)}$ and mineral composition of APGPRGs, ANDSRGs and CBGPRGs

Row	Rock group	ρ (g/cm^3)			UCS (MPa)			$I_{s(50)(Axial)}$ (MPa)			$I_{s(50)(Diametral)}$ (MPa)			Mineral composition%		
		Dry	Sat	%	(Dry)	(Sat)	%	(Dry)	(Sat)	%	(Dry)	(Sat)	%	GP	AN	CMs
Almost pure gypsum																
1	KG1-1	2.08	2.28	9.71	25.72	9.65	−62.48	1.81	0.74	−59.12	2.16	0.88	−59.26	91.31	1.60	7.10
2	TG1-1	2.27	2.29	0.91	22.42	14.72	−34.34	1.66	0.71	−57.23	1.37	0.93	−32.12	93.04	1.33	5.62
3	TG2-1	2.26	2.29	1.37	23.11	15.70	−32.06	1.75	0.87	−50.29	1.34	0.62	−53.73	93.92	1.52	4.65
Mean		2.20	2.29	4.00	23.75	13.36	−42.96	1.74	0.77	−55.54	1.62	0.81	−48.37	92.76	1.48	5.79
St.D		0.11	0.00	4.95	1.74	3.25	16.94	0.08	0.09	4.65	0.47	0.17	14.34	1.33	0.14	1.23
Anhydrite dominant sulfate rocks																
1	KG3-1	2.64	2.70	2.19	33.47	31.62	−5.53	2.54	1.96	−22.83	2.22	2.15	−3.15	20.27	75.27	4.46
2	MG3-1	2.63	2.64	0.45	33.10	30.71	−7.22	2.88	2.18	−24.31	2.72	2.58	−5.15	18.73	81.27	0.00
3	MG4-5	2.67	2.69	0.49	52.04	46.35	−10.93	3.24	2.81	−13.27	3.51	2.68	−23.65	29.07	69.16	1.77
4	MG2-2	2.54	2.54	0.12	34.47	24.88	−27.82	2.33	1.84	−21.03	3.01	2.54	−15.61	23.94	71.44	4.63
Mean		2.62	2.64	0.81	38.27	33.39	−12.88	2.75	2.20	−20.36	2.87	2.49	−11.89	23.00	74.28	2.71
St.D		0.06	0.07	0.93	9.20	9.14	10.22	0.40	0.43	4.91	0.54	0.23	9.55	4.59	5.29	2.23
Clay bearing gypsum																
1	KA1-2	2.21	2.22	0.45	27.30	21.46	−21.39	1.75	0.97	−44.57	1.64	0.87	−46.95	68.89	1.70	29.41
2	KG2-1	2.27	2.28	0.53	34.73	20.51	−40.94	2.25	0.77	−65.78	2.01	1.06	−47.26	70.38	0.38	29.23
Mean		2.24	2.25	0.49	31.02	20.99	−31.17	2.00	0.87	−55.17	1.83	0.97	−47.11	69.64	1.04	29.32
St.D		0.05	0.05	0.06	5.25	0.67	13.83	0.35	0.14	15.00	0.26	0.13	0.22	1.05	0.93	0.12

Similar values in the dry conditions of the ANDSRG samples are 38.27 ± 9.20, 2.75 ± 0.40, 2.87 ± 0.54 MPa and in the saturated conditions, 33.39 ± 9.14, 2.20 ± 0.43 and 2.49 ± 0.23 MPa. The reduction effect of saturation on the mean UCS, $I_{s(50)(Axial)}$ and $I_{s(50)(Diametral)}$ of APGPRG samples are 42.96 ± 16.94, 55.54 ± 4.65 and 48.37 ± 14.34 %, respectively, and ANDSRG samples are 12.88 ± 10.22, 20.36 ± 4.91 and 11.89 ± 9.55%. These results show that

the water softening effect on the three strength properties experienced in this research in APGPRG samples (weaker rocks), is much greater than ANDSRG samples (stronger rocks). The mean UCS, $I_{s(50)(Axial)}$ and $I_{s(50)(Diametral)}$ samples of the two CBGPRGs in dry conditions are 31.02 ± 5.25, 2.0 ± 0.35 and 1.87 ± 0.26 MPa, and in saturated conditions are 20.99 ± 0.67, 0.87 ± 0.14 and 0.97 ± 0.13 MPa, respectively. Comparison of the test results of CBGPRG samples with APGPRG samples shows the strengthening effect of clay-sized minerals on the strength properties of APGPRG samples. Such an increase can be attributed to the carbonate (calcite and dolomite) nature of the clay-sized particles in this study's matrix of these experienced rocks. The average UCS of calcite and dolomite in dry conditions is about 60 MPa, while gypsum is about 20 to 40 MPa.

In Table 8, the ratios between $UCS_{(Dry)}/I_{s(50)(Axial)(Dry)}$, $UCS_{(Sat)}/I_{s(50)(Axial)(Sat)}$, $UCS_{(Dry)}/I_{s(50)(Diametral)(Dry)}$, $UCS_{(Sat)}/I_{s(50)(Diametral)(Sat)}$, $I_{s(50)(Axial)(Dry)}/I_{s(50)(Diametral)(Dry)}$, $I_{s(50)(Axial)(Sat)}/I_{s(50)(Diametral)(Sat)}$ are presented as conversion factors $K_{1(Dry)}$, $K_{1(Sat)}$, $K_{2(Dry)}$, $K_{2(Sat)}$, $K_{3(Dry)}$ and $K_{3(Sat)}$ for all different rock groups in dry and saturated conditions, respectively.

Table 8 Conversion factors of $I_{s(50)(Axial)} - I_{s(50)(Diametral)}$ to UCS and $I_{s(50)(Diametral)}$ to $I_{s(50)(Axial)}$ for each rock group

Row	Rock group	UCS/ $I_{s(50)(Axial)}$		UCS/ $I_{s(50)(Diametral)}$		$I_{s(50)(Axial)}$/ $I_{s(50)(Diametral)}$	
		$K_{1(Dry)}$	$K_{1(Sat)}$	$K_{2(Dry)}$	$K_{2(Sat)}$	$K_{3(Dry)}$	$K_{3(Sat)}$
1	KA1-2	15.60	22.12	16.65	24.67	1.07	1.11
2	KA2-1	29.63	20.76	24.17	12.69	0.82	0.61
3	KG1-1	14.21	13.04	11.91	10.97	0.84	0.84
4	KG2-1	15.44	26.64	17.28	19.35	1.12	0.73
5	KG3-1	13.18	16.13	15.08	14.71	1.14	0.91
6	KG4-1	17.81	19.54	17.30	13.33	0.97	0.68
7	MG1-2	18.30	18.84	24.27	23.55	1.33	1.25
8	MG2-1	10.59	22.44	11.00	15.78	1.04	0.70
9	MG2-2	14.79	13.52	11.45	9.80	0.77	0.72
10	MG3-1	11.49	14.09	12.17	11.90	1.06	0.84
11	MG4-2	18.82	22.59	16.24	17.30	0.86	0.77
12	MG4-5	16.06	16.49	14.83	17.29	0.92	1.05
13	NG1-1	13.51	19.43	19.33	23.93	1.43	1.23
14	NG2-1	12.14	15.44	14.94	18.34	1.23	1.19
15	NG2-2	13.53	12.27	12.75	14.09	0.94	1.15
16	TG1-1	13.51	20.73	16.36	15.83	1.21	0.76
17	TG2-1	13.21	18.05	17.25	25.32	1.31	1.40
Mean		4.21	4.47	16.06	16.99	1.06	0.94
Max		5.74	6.39	24.27	25.32	1.43	1.40
Min		3.02	2.09	11.00	9.80	0.77	0.61
St.D		0.78	1.14	3.89	4.93	0.19	0.24

In Table 9, the values of these conversion factors are presented only for APGPRGs, ANDSRGs and CBGPRGs. The values of $I_{s(50)(Axial)}$ conversion factor to UCS for APGPRGs in dry ($K_{1(Dry)}$) and saturated ($K_{1(Sat)}$) conditions are 13.64 ± 0.52 and 17.27 ± 3.90, respectively, and for ANDSRGs are 13.88 ± 1.98 and 15.06 ± 1.47. The conversion factor of $I_{s(50)(Diametral)}$ to UCS for APGPRGs in dry ($K_{2(Dry)}$) and saturated ($K_{2(Sat)}$) conditions are 15.17 ± 2.86 and 17.37 ± 7.30 and for ANDSRGs 13.38 ± 1.84 and 13.43 ± 3.27, respectively. Comparison of CBGPRGs conversion factors with APGPRGs also shows the increasing effect of carbonated clay-sized minerals on the conversion factors. The values of the conversion factors obtained for converting the APLI and DPLI to UCS for the three types of sulfate rocks (APGPRGs, ANDSRGs and CBGPRGs) show that the values of these conversion factors are much lower than the overall conversion factor of 24 reported by Broch and Franklin [3] and Bieniawski [5] for different types of rocks and therefore the use of above conversion factor can cause up to 80% error in estimating UCS (magnification) of sulfate rocks based on the point load test results. Comparison of the ratio between $I_{s(50)(Axial)}/I_{s(50)(Diametral)}$ in dry ($K_{3(Dry)}$) and saturated ($K_{3(Sat)}$) conditions for all three groups of rocks shows that the value of this ratio is average in the range of 1 or slightly more than 1. This means that the conversion factors of $I_{s(50)(Axial)(Dry)}$ and $I_{s(50)(Diametral)}$ to UCS in the studied sulfate rocks were very close to each other.

In Fig. 8, the correlation between the conversion factors of $I_{s(50)(Axial)} - I_{s(50)(Diametral)}$ to UCS (*Y*-axis) with the mineral composition of rock groups (*X*-axis), for 14 rock groups consisting of GP and AN (CMs < 5%) is presented in dry (Fig. 8 (a)) and saturated (Fig. 8 (b)) conditions. To eliminate the amount of CMs content in the mineral composition of rock groups with less than 5% of CMs, the amount of clay-sized minerals was removed from 100% mineral compositions, and then the share of each GP and AN was recalculated from 100%. In Fig. 8, on the *x*-axis, the amount of GP increases from right to left and the amount of AN increases from right to left. In both Fig. 8 (a) and (b), the best-fitted curves of linear type with very low determination coefficients only show an increase in each of the $K_{1(Dry)}$, $K_{2(Dry)}$, $K_{1(Sat)}$ and $K_{1(Sat)}$ factors by increasing the amount of GP in a sulfate rock composed of GP – AN and in fact confirming the increase in the amount of these factors, by weakening the rock in both dry (Eqs. (4) and (5)) and saturation (Eqs. (6) and (7)) conditions.

Table 9 Conversion factors of $I_{s(50)(Axial)} - I_{s(50)(Diametral)}$ to UCS for APGPRGs, ANDSRGs and CBGPRGs in dry and saturated conditions

Texture	Number of sample series	Statistical functions	ρ (g/cm^3)	UCS (MPa)	$I_{s(50)(Axial)}$ (MPa)	$I_{s(50)(Diametral)}$ (MPa)	GP%	AN%	CMs%
Almost pure gypsum (GP > 90%)(AN < 5%)(CMs < 5%)									
Dry condition									
Alabaster	18	Mean	2.27	24.69	1.77	1.44	96.02	1.19	2.84
		St.D	0.02	7.70	0.39	0.37	1.46	1.46	0.88
Sat condition									
Alabaster	16	Mean	2.30	15.08	0.80	0.90	96.27	1.08	2.78
		St.D	2.28	9.61	0.37	0.19	94.00	0.00	1.04
Anhydrite dominant (GP < 27%)(AN > 70%)(CMs < 5%)									
Dry condition									
Porphyry	38	Mean	2.60	38.36	2.75	2.86	22.93	75.40	1.67
		St.D	0.08	12.12	0.61	0.76	4.81	5.47	1.21
Sat condition									
Porphyry	21	Mean	2.65	35.58	2.22	2.62	22.90	75.71	1.40
		St.D	0.09	11.74	0.61	0.62	6.19	6.80	1.02
Clay bearing gypsum (GP > 60%)(AN < 5%)(25 < CMs < 36%)									
Dry condition									
Alabaster	9	Mean	2.34	31.55	1.91	1.85	62.83	3.08	34.09
		St.D	0.07	6.27	0.55	0.60	3.70	1.11	2.59
Porphyry	11	Mean	2.27	34.43	2.14	1.98	70.31	0.54	29.15
		St.D	0.02	7.34	0.36	0.75	1.74	0.62	2.25
Sat condition									
Alabaster	9	Mean	2.29	25.22	1.05	0.95	63.46	2.78	33.77
		St.D	0.02	7.35	0.21	0.23	4.01	1.43	2.64
Porphyry	19	Mean	2.26	20.18	0.92	1.28	71.05	0.23	28.71
		St.D	0.03	4.34	0.52	0.41	1.53	0.43	1.48

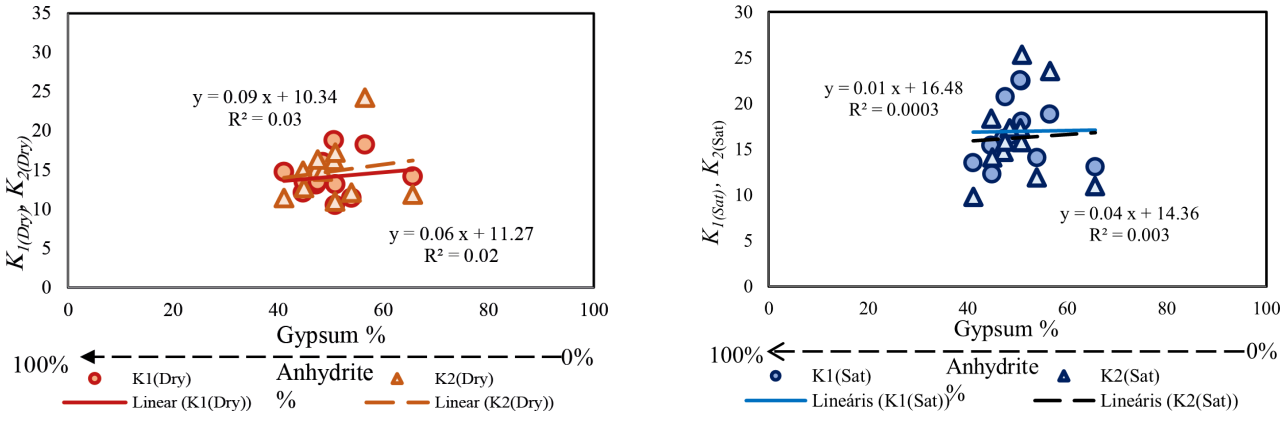

Fig. 8 Correlation between the conversion factors of $I_{s(50)(Axial)} - I_{s(50)(Diametral)}$ to UCS with the mineral composition of rock groups in (a) dry and (b) saturated conditions

$$K_{1(Dry)} = 0.06\ GP\% + 11.27 \quad R^2 = 0.02 \tag{4}$$

$$K_{2(Dry)} = 0.09\ GP\% + 10.34 \quad R^2 = 0.03 \tag{5}$$

$$K_{1(Sat)} = 0.04\ GP\% + 14.36 \quad R^2 = 0.01 \tag{6}$$

$$K_{1(Sat)} = 0.01\ GP\% + 16.48 \quad R^2 = 0.01 \tag{7}$$

5.2 Analysis based on the mineral composition of all samples

In this type of analysis, regardless of the sampling location of rock blocks, 182 series of triple-tested samples were divided into three main groups, a series of rock samples consisting of almost pure gypsum (GP > 90%, AN < 5% and CMs < 5%, refer to APGPMRG), anhydrite dominant (GP < 27%, AN > 70%, CMs < 5% refer to ANDSRMG) and clay-sized bearing gypsum (GP > 60%, AN < 5% and 25 < CMs < 36% refer to CMBGPMRG) rock groups in terms of mineral composition. Based on this classification, 34 (18 alabaster textures and 16 porphyry textures), 59 (all porphyry textures) and 20 (9 alabaster textures and 11 porphyry textures) sample series were divided into three main groups, respectively. A number of tested series could not be used in this type of analysis due to their mineral composition contrary to the three specified levels of classification. Due to the present the results of each series of samples in Appendices A and B, in Table 10 only the UCS, $I_{s(50)(Axial)}$ and $I_{s(50)(Diametral)}$ obtained statistical functions for each group is presented. Comparison of the mean values in Table 10 with Table 7 shows that except for three cases (with an increase of about 3 to 11%), in all other cases, the use of samples taken from different locations, led to a decrease in the three studied strength properties, from about 1% to 32%.

In Table 10, the mean UCS, $I_{s(50)(Axial)}$, $I_{s(50)(Diametral)}$, the mineral composition of APGPMRG, ANDSRMG and CMBGPMRG samples are presented in dry and saturated conditions. APGPMRG includes 18 series of UCT, APLT and DPLT samples that tested in dry conditions and 16 series in saturated conditions, all with alabaster texture. The mean UCS, $I_{s(50)(Axial)}$, $I_{s(50)(Diametral)}$ of alabaster APGPMRG samples are 24.69 ± 7.70, 1.77 ± 0.39 and 1.44 ± 0.37 MPa in dry conditions and 15.08 ± 9.61, 0.80 ± 0.37 and 0.90 ± 0.19 MPa in saturated conditions, respectively. Saturation has resulted in 39, 55 and 37% reduction in three strength indices, respectively. All of the

Table 10 Mean UCS, $I_{s(50)(Axial)}$ and $I_{s(50)(Diametral)}$ statistical functions and mineral composition of APGPMRG, ANDSRMG and CMBGPMRG samples tested in dry and saturated conditions

Texture	Number of sample series	Statistical functions	ρ (g/cm^3)	UCS (MPa)	$I_{s(50)(Axial)}$ (MPa)	$I_{s(50)(Diametral)}$ (MPa)	GP%	AN%	CMs%
Almost pure gypsum (GP > 90%)(AN < 5%)(CMs < 5%)									
Dry condition									
Alabaster	18	Mean	2.27	24.69	1.77	1.44	96.02	1.19	2.84
		St.D	0.02	7.70	0.39	0.37	1.46	1.46	0.88
Sat condition									
Alabaster	16	Mean	2.30	15.08	0.80	0.90	96.27	1.08	2.78
		St.D	2.28	9.61	0.37	0.19	94.00	0.00	1.04
Anhydrite dominant (GP < 27%)(AN > 70%)(CMs < 5%)									
Dry condition									
Porphyry	38	Mean	2.60	38.36	2.75	2.86	22.93	75.40	1.67
		St.D	0.08	12.12	0.61	0.76	4.81	5.47	1.21
Sat condition									
Porphyry	21	Mean	2.65	35.58	2.22	2.62	22.90	75.71	1.40
		St.D	0.09	11.74	0.61	0.62	6.19	6.80	1.02
Clay bearing gypsum (GP > 60%)(AN < 5%)(25 < CMs < 36%)									
Dry condition									
Alabaster	9	Mean	2.34	31.55	1.91	1.85	62.83	3.08	34.09
		St.D	0.07	6.27	0.55	0.60	3.70	1.11	2.59
Porphyry	11	Mean	2.27	34.43	2.14	1.98	70.31	0.54	29.15
		St.D	0.02	7.34	0.36	0.75	1.74	0.62	2.25
Sat condition									
Alabaster	9	Mean	2.29	25.22	1.05	0.95	63.46	2.78	33.77
		St.D	0.02	7.35	0.21	0.23	4.01	1.43	2.64
Porphyry	19	Mean	2.26	20.18	0.92	1.28	71.05	0.23	28.71
		St.D	0.03	4.34	0.52	0.41	1.53	0.43	1.48

ANDSRMG sample series in dry and saturated conditions have porphyry texture and their mean UCS, $I_{s(50)(Axial)}$, $I_{s(50)(Diametral)}$ in dry conditions are 38.36 ± 12.12, 2.75 ± 0.61 and 2.86 ± 0.76 MPa and in saturation conditions, 35.58 ± 11.74, 2.22 ± 0.61 and 2.62 ± 0.62 MPa, respectively, and saturation caused 7, 19 and 18% decrease in the three strength indices, respectively. Saturation results in two different tested APGPMRG and ANDSRMG series of samples show that the weakening effect of water on weaker rocks is greater than stronger rocks. Also, the mean values of UCS, $I_{s(50)(Axial)}$, $I_{s(50)(Diametral)}$ of the porphyry ANDSRMG sample series in dry conditions are 55, 55 and 98%, respectively, and in saturated conditions 136, 178 and 191% and more than the alabaster APGPMRG sample series is similar conditions. Compared to the alabaster APGPMRG sample series means, the CMBGPMRG sample series in dry conditions have 28, 7 and 28% higher UCS, $I_{s(50)(Axial)}$, $I_{s(50)(Diametral)}$ means, respectively. As mentioned before, the reason for such an increase can be attributed to the presence of clay-sized carbonate particles (calcite and dolomite) with higher strength than GP in the rock matrix. This increase in strength is also seen in clay-bearing gypsum in saturated conditions. Measurement of the penetration of steel conical platens during axial point load tests showed that in oven-dried and saturated samples, the penetration amount of alabaster APGPMRG samples is 2.36 and 1.23 mm, and in ANDSRMG samples is 1.44 and 1.01 mm. Such penetration values indicate that, firstly, the penetration amount of alabaster APGPMRG samples is higher than the ANDSRMG samples. Second, the penetration in saturated conditions is less than in the dry condition (contrary to expectations). The reason for this seems to be a greater reduction in the strength of the rock than the frictional resistance at the point of penetration of the tip of the steel conical platens in the saturated condition. In fact, before the conical platens tips can penetrate more into the sample, the sample breaks. The penetration values in the DPLTs in APGPMRG samples in dry and saturated conditions are 2.48 and 2.61 mm, respectively, and in the ANDSRMG samples are 3.17 and 4.66 mm. In DPLT samples, although the penetration amount in the ANDSRMG samples is expected to be less than in the APGP samples, the opposite is observed. This seems to be due to the greater strength of the ANDSRMG specimens at a thickness close to the specimen diameter and the need for more steel conical platens to try to break the specimen. Given the inverse relationship between De and I_s in the equation $I_s = P/De^2$, It can be concluded that not measuring the amount of penetration in the PLTs and using the initial thickness or diameter of the sample can lead to a smaller erroneous calculation for I_s in week rocks.

Regression analysis of the UCTs, APLTs and DPLTs results of series of samples placed in three main rock groups in dry and saturated conditions (for example, Fig. 9 for a series of ANDSRMG samples) led to relationships of Eqs. (8)–(11) (for alabaster APGPMRG series of samples), Eqs. (12)–(15) (for porphyry ANDSRMG series of samples), Eqs. (16)–(19) (for alabaster CMBGPMRG series of samples) and Eqs. (20)–(23) (for porphyry CMBGPMRG series of samples) for the three main rock groups rock, respectively, in dry and saturated conditions:

- for $APGPMRG_{(Alabaster)}$:

$$UCS_{(Dry)} = 11.68\ I_{s(50\%)(Axial)(Dry)}^{1.92} \quad R^2 = 0.94 \tag{8}$$

$$UCS_{(Dry)} = 15.90\ I_{s(50\%)(Diametral)(Dry)}^{1.17} \quad R^2 = 0.91 \tag{9}$$

$$UCS_{(Sat)} = 13.99\ I_{s(50\%)(Axial)(Sat)} + 4.67 \quad R^2 = 0.94 \tag{10}$$

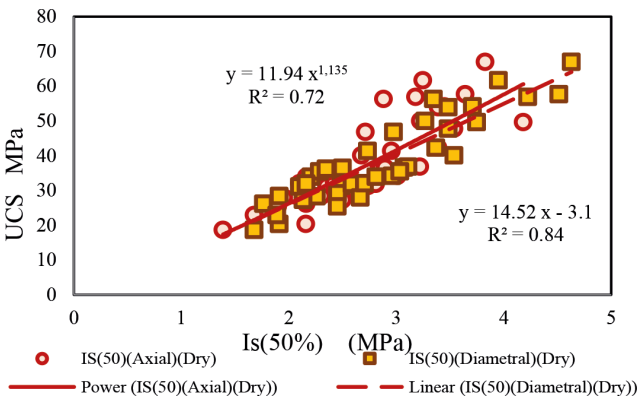

(a)

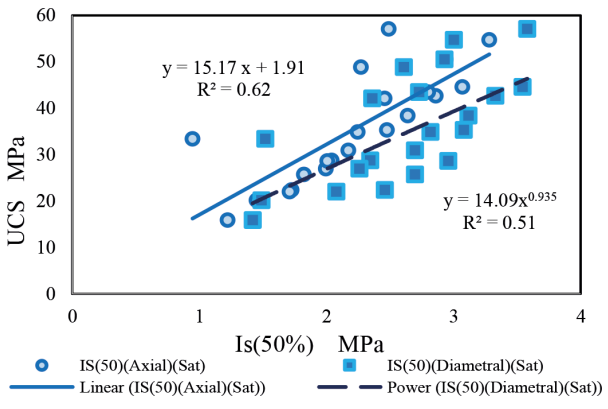

(b)

Fig. 9 Correlation between UCTs, APLTs and DPLTs results for ANDSRMG in (a) dry, (b) saturated condition

$$UCS_{(Dry)} = 6.22\ I_{s(50\%)(Diametral)(Sat)} + 9.51 \quad R^2 = 0.84 \tag{11}$$

- for $ANDSRMG_{(Porphyry)}$:

$$UCS_{(Dry)} = 11.94\ I_{s(50\%)(Axial)(Dry)}^{1.14} \quad R^2 = 0.72 \tag{12}$$

$$UCS_{(Dry)} = 14.52\ I_{s(50\%)(Diametral)(Dry)} - 3.10 \quad R^2 = 0.84 \tag{13}$$

$$UCS_{(Sat)} = 15.17\ I_{s(50\%)(Axial)(Sat)} + 1.91 \quad R^2 = 0.63 \tag{14}$$

$$UCS_{(Dry)} = 14.09\ I_{s(50\%)(Diametral)(Sat)}^{0.94} \quad R^2 = 0.51 \tag{15}$$

- for $CMBGPMRG_{(Alabaster)}$:

$$UCS_{(Dry)} = 11.04\ I_{s(50\%)(Axial)(Dry)} + 10.47 \quad R^2 = 0.92 \tag{16}$$

$$UCS_{(Dry)} = 22.48\ I_{s(50\%)(Diametral)(Dry)}^{0.57} \quad R^2 = 0.91 \tag{17}$$

$$UCS_{(Sat)} = 37.71\ I_{s(50\%)(Axial)(Sat)} - 15.20 \quad R^2 = 0.92 \tag{18}$$

$$UCS_{(Dry)} = 29.09\ I_{s(50\%)(Diametral)(Sat)} - 1.51 \quad R^2 = 0.86 \tag{19}$$

- for $CMBGPMRG_{(Porphyry)}$:

$$UCS_{(Dry)} = 17.84\ I_{s(50\%)(Axial)(Dry)} - 3.82 \quad R^2 = 0.77 \tag{20}$$

$$UCS_{(Dry)} = 9.70\ I_{s(50\%)(Diametral)(Dry)} + 15.27 \quad R^2 = 0.98 \tag{21}$$

$$UCS_{(Sat)} = 21.27\ I_{s(50\%)(Axial)(Sat)}^{0.34} \quad R^2 = 0.60 \tag{22}$$

$$UCS_{(Dry)} = 17.90\ I_{s(50\%)(Diametral)(Sat)}^{0.54} \quad R^2 = 0.65. \tag{23}$$

Since most of the series of alabaster APGPMRG samples are the same as APGPRG rock group samples, so the obtained determination coefficients values for the APGPMRG sample series are in the range of mean determination coefficients values for the APGPRG rock group (the axial and diametral equations for dry and for saturation conditions are in the rows 3, 16 and 17 of Table 5) relationships. However, in most of the similar equations obtained for ANDSRMG and CMBGPMRG, the values of the determination coefficients are reduced. This means that even if the mineral composition of the samples is the same, if the rock blocks are taken from different locations, the value of the determination coefficients and the reliability of the extracted equations between the PLI and the UCS of the sulfate rock are reduced for use in UCS forecasts. In Fig. 9, there is a weaker correlation between UCS and $I_{s(50)}$ in saturated conditions rather than dry conditions. It can be caused by the absorption of water in the layered structure of silicates in clay minerals and the angle of placement of these layered structures in relation to the loading direction.

5.3 Deformation and type of failure in point load tests

Deformation of rocks under normal loads is a function of lithological characteristics, grain size, internal structure, the pattern of loads, etc. So far, most of the deformation curves presented for GP and AN in the UCT are S-shaped and usually have three stages: plastic, elastic and plastic [79–81]. Therefore, basically, the deformation behavior of these two rocks under loads is usually plastic-elastic-plastic. However, so far, no research has been done on the deformation behavior of rocks during point load testing. In order to investigate the behavior of sulfate rock samples during APLTs and DPLTs, as mentioned above, by installing a strain gauge with an accuracy of 0.001 mm on the lower metal platform of the UCT instrument (Fig. 10), the penetration rate of the metal cones, as well as the deformation of the loading points of specimens in the direction of loading, was recorded (Fig. 11). With gradual increasing of the load on the sample, the amount of point load strength gradually increases and in proportion to the strength of the rock, after reaching the peak strength, the sample will failure. In order to obtain deformation curve and failure mode, a correlation was established between the instantaneous

Fig. 10 Installing the strain gauge on the metal plate located on the loading platform below the samples

Fig. 11 Local failure during point load tests

thickness of the specimens (D') and the instantaneous point load index ($I_{s(50)\text{Instantaneous}}$) during the experiments for all specimens. In fact, the created correlation is similar to the stress-strain correlation in UCT, but instead of using strain, the instantaneous thickness of PLT specimens is used during the tests. Such a correlation has not been observed in the thematic literature and taken as an initiative in this article. The creation of such correlations leads to different "instantaneous thickness-instantaneous PLI" curves for different types of sulfate rocks (Fig. 12).

Brittle elastic deformation was observed in porphyry anhydrite dominant samples (such as KG3-1, MG2-2, MG3-1 and MG4-5 groups). In such rocks, with a gradual increasing the load, the rock suddenly (Fig. 12 (a)) or after one to several local failures at the point of penetration of metal cones, becomes failure (Fig. 12 (b), (c) and (d)). In this type of rocks, although the deformation of the rock sample under the point load test is an elastic type, but with the continuous crushing of a number of porphyry crystals in the rock sample, the complete failure of the sample is faced with delays. However, the predominant behavior in almost pure gypsum specimens is elastoplastic deformation. This type of deformation is the dominant behavior in many samples, including samples with high GP content with porphyry texture such as KG1-1 and alabaster texture of all rock groups belonging to the Kangir and Nargesi dam sites, as well as some porphyry anhydride dominant samples such as KG3-1, MG1-2, MG3-1, MG4-2 and MG4-5 rock groups. This type of deformation is observed in different forms of one to several-stage rupture (Fig. 12 (c), (f), (g), (h)). The rupture in this type of rock is mainly brittle.

In some samples, with increasing load on the specimen, there is initially no penetration (or very small or limited penetration), but after increasing the load, the elastic behavior with one-stage (Fig. 12 (i)), two-stages (Fig. 12 (j)), three stages (Fig. 12 (k)) to several stages (Fig. 12 (l)) brittle failure are observed. In fact, the rock sample at the applied load, at first resisted to a degree commensurate with the hardness and strength of the rock, but after increasing the amount of load from the resistance point (Resistance of rock particles to crushing or resistance due to adhesion created between rock particles due to the matrix), penetrate to the sample begins and then the path of elastic deformation goes through and eventually leads to brittle failure. This type of deformation can be called "elastic deformation with initial strength stiffness" or "elastic deformation with pre-strength stiffness". Such deformation was seen in some samples containing high GP content with alabaster texture such as NG1-1, and with porphyry texture such as KG1-1 or porphyry anhydride dominant such as KG2-1, MG2-2, MG4-2, 5.

In some AN dominant sulfate rock samples with porphyry texture such as KG2-1, KG3-1, MG1-2, MG2-1, MG3-1 and MG4-2,5 as well as almost pure GP samples with porphyry texture such as KG1-1 and alabaster textures such as NG1-1, NG2-1, TG1-1 and TG2-1 show elastic-plastic-elastic deformation in which the initial deformation of the rock is elastic and then after a stage of plastic behavior, re-entered the elastic behavior and brittle failure (Fig. 12 (m), (n)). In a very limited number of samples, the sample is failure after reaching the peak strength, but if the experiment continues, some residual strength is observed (Fig. 12 (o)) due to the plastic deformation of the pressed material under the metal cones. This type of deformation can be described as "elastoplastic deformation with temporary residual strength". Such deformation and failure were observed in some samples containing significant clay mineral content with porphyry texture such as KG2-1 and also samples with high alabaster gypsum such as NG1-1, NG2-1, NG2-2, TG1-1 and TG2-1. Therefore, very different deformation behavior can be observed during point load tests depending on the mineral composition of sulfate rocks.

6 Conclusions

Although axial and diametral point load testing to predict the uniaxial compressive strength is common in many civil projects today, research on sulfate rocks has been very limited. In this study, focusing on sulfate rocks with different mineral compositions, it was concluded that:

1. There is a unique relationship between the axial – diametral point load index and the UCS for each specific mineral composition.

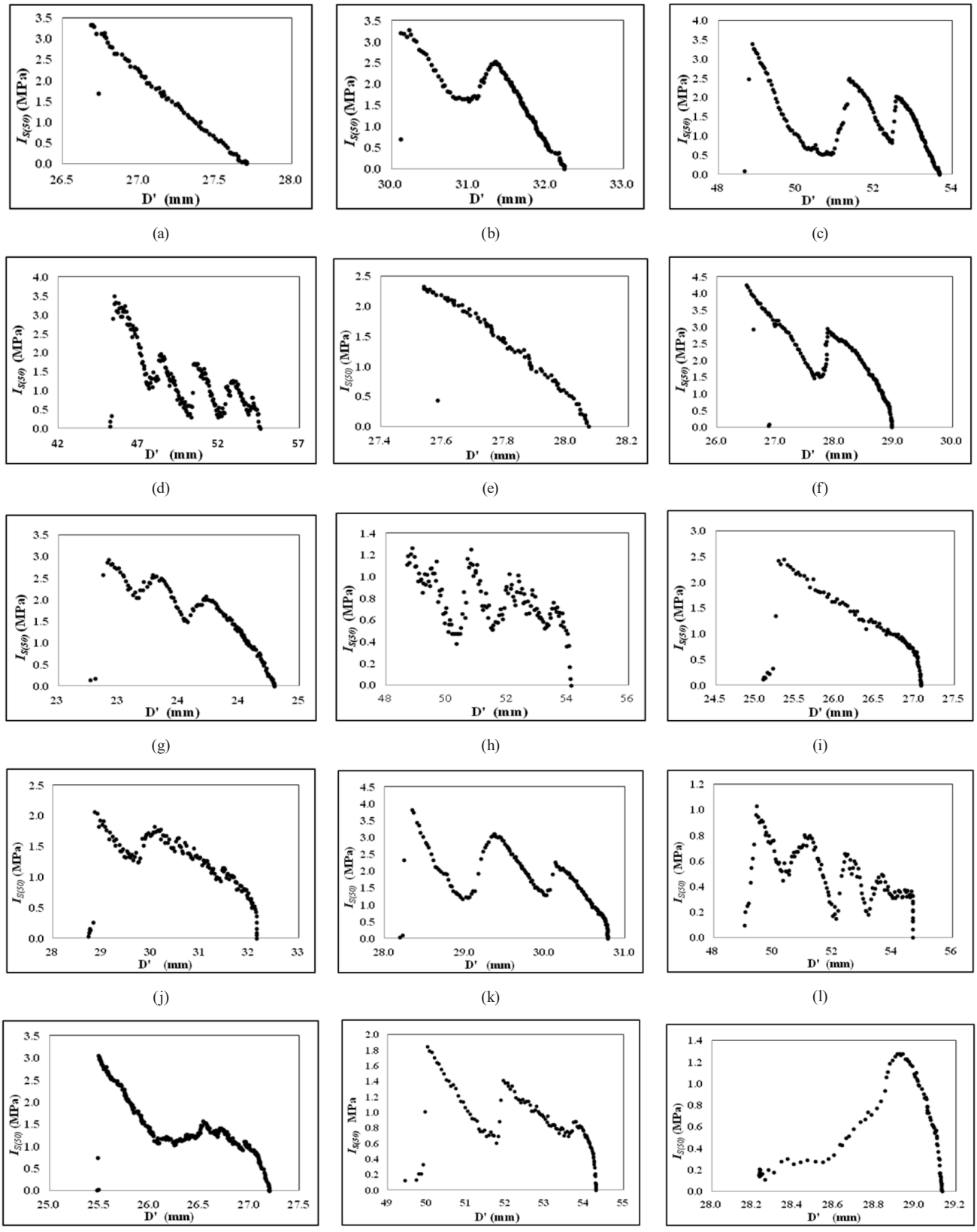

Fig. 12 The point load tests "Thickness-Is(50%)" curves with deformation: 1 - Elastic with (a) single-stage, (b) double stage, (c) triple stage, (d) Multi-stage brittle failure; 2 - Elastoplastic with (e) single-stage, (f) double stage, (g) triple stage, (h) multi-stage brittle failure, 3 - Elastic with initial pre-hardening and (i) one-stage, (j) double stage, (k) triple stage, (l) multi-stage brittle failure, 4 - Elastic-plastic-elastic with (m) double stage, (n) triple stage brittle failure; 5 - Elastoplastic with residual strength (o) one stage

2. The mean UCS, $I_{s(50)(Axial)}$ and $I_{s(50)(Diametral)}$ of almost pure gypsum samples in dry conditions are 23.75 ± 1.74, 1.74 ± 0.08 and 1.62 ± 0.47 MPa, respectively, and in saturated conditions, 13.36 ± 3.25, 0.77 ± 0.09 and 0.81 ± 0.17 MPa. Similar values in the dry conditions of the anhydrite dominant samples are 38.27 ± 9.20, 2.75 ± 0.40, 2.87 ± 0.54 MPa and in the saturated conditions, 33.39 ± 9.14, 2.20 ± 0.43 and 2.49 ± 0.23 MPa.
3. The values of $I_{s(50)(Axial)}$ conversion factor to UCS for almost pure gypsum samples in dry conditions and saturated are 13.64 ± 0.52 and 17.27 ± 3.90, respectively, and for anhydrite dominant samples are 13.88 ± 1.98 and 15.06 ± 1.47. The conversion factor of $I_{s(50)(Diametral)}$ to UCS for almost pure gypsum samples in dry and saturated conditions are 15.17 ± 2.86 and 17.37 ± 7.30 and for anhydrite dominant samples 13.38 ± 1.84 and 13.43 ± 3.27, respectively. Therefore, the conversion factors of point load indices to UCS in sulfate rocks are far less than the value of 24 announced by some authors for different rocks.
4. Comparison of the ratio between $I_{s(50)(Axial)}/I_{s(50)(Diametral)}$ in dry and saturated conditions for studied sulfate rocks shows that the value of this ratio is average in the range of 1 or slightly more than 1.
5. The results of axial and diametral point load tests can be used with the same reliability to predict the UCS.
6. If rock samples with the same mineral composition are gathered from different geographical or geological points, the reliability of the equations obtained between point load indices and UCS, will face with a significant reduction compared to samples taken from a unique location. Therefore, such correlations are better to be done independently for samples taken from each sampling site.
7. The obtained results of the point load test on sulfate rocks show very different deformation behavior such as elastic, elastoplastic, elastic deformation with initial strength stiffness, elastic-plastic-elastic, elastic deformation with pre-strength stiffness, elastoplastic deformation with temporary residual strength, before failure.

The results obtained above regarding uniaxial compressive strength, axial and diagonal point load strength, as well as correlation relations for almost pure gypsum and anhydrite predominant sulfated rocks can be used with sufficient reliability in other similar researches. But as mentioned above, for each special geological and geographical situation, especially in development plans, it is necessary to conduct special tests on rock samples.

Authors' contributions

Mohammad Reza Rahimi: Conceptualization, Visualization, Methodology, Investigation, Data curation; Formal analysis, Writing - original draft, Resources; Seyed Davoud Mohammadi: Supervision, Review & editing, Funding acquisition.

Funding

This work was supported by the vice-president research office of Bu-Ali Sina University, Iran [grant number 4.95].

Acknowledgements

A grant-funded this research to authors by the vice-president research office of Bu-Ali Sina University, Iran, is gratefully acknowledged. Also, preparation of rock samples and conducting experiments were undertaken in the Engineering Geological and Geotechnical Laboratory of Bu-Ali Sina University. Therefore, thanks and appreciation for the contributions made in this field.

References

[1] ISRM "Suggested method for determining point load strength: ISRM Comm on testing methods Int J Rock Mech Min SciV22, N2, April 1985, P51–60", International Journal of Rock Mechanics and Mining Sciences & Geomechanical Abstracts, 22(4), p. 112, 1985. https://doi.org/10.1016/0148-9062(85)92985-7

[2] ASTM "ASTM D5731-16 Standard Test Method for Determination of the Point Load Strength Index of Rock and Application to Rock Strength Classifications", ASTM International, West Conshohocken, PA, USA, 2016. https//doi.org/10.1520/D5731-16

[3] Broch, E., Franklin, J. A. "The point-load strength test", International Journal of Rock Mechanics and Mining Sciences & Geomechanical Abstracts, 9(6), pp. 669–676, 1972. https://doi.org/10.1016/0148-9062(72)90030-7

[4] Guidicini, G., Nieble, C. M., de Cornides, A. T. "Analysis of point load test as a method for preliminary geotechnical classification of rocks", Bulletin of the International Association of Engineering Geology, 7(1), pp. 37–52, 1973. https://doi.org/10.1007/BF02635318

[5] Bieniawski, Z. T. "The point-load test in geotechnical practice", Engineering Geology, 9(1), pp. 1–11, 1975. https://doi.org/10.1016/0013-7952(75)90024-1

[6] Brook, N. "Size correction for point-load testing", International Journal of Rock Mechanics and Mining Sciences & Geomechanical Abstracts, 17(4), pp. 231–235, 1980. https://doi.org/10.1016/0148-9062(80)91090-6

[7] Greminger, M. "Experimental studies of the influence of rock anisotropy on size and shape effects in point-load testing", International Journal of Rock Mechanics and Mining Sciences & Geomechanical Abstracts, 19(5), pp. 241–246, 1982. https://doi.org/10.1016/0148-9062(82)90222-4

[8] Forster, I. R. "The influence of core sample geometry on the axial point-load test", International Journal of Rock Mechanics and Mining Sciences & Geomechanical Abstracts, 20(6), pp. 291–295, 1983. https://doi.org/10.1016/0148-9062(83)90599-5

[9] D'Andrea, D. V., Fisher, R. L., Fogelson, D. E. "Prediction of compression strength from other rock properties", U.S. Department of the Interior, Bureau of Mines, Washington, DC, USA, Rep. 6702, 1965.

[10] Reichmuth, D. R. "Point load testing of brittle materials to determine tensile strength and relative brittleness", In: Grosvener, N. E., Paulding, B. W. (eds.) Proceedings of the 9th U.S. Symposium on Rock Mechanics, Port City Press, Baltimore, MD, USA, 1968, pp. 134–159.

[11] Pells, P. J. N. "The use of point load test in predicting the compressive strength of rock material", Australian Geomechanics Journal, G5(1), pp. 54–56, 1975.

[12] Deere, D. U., Miller, R. P. "Engineering classification and index properties of intact rock", University of Illinois, Urbana, IL, USA, Technical report No. AFWL-TR, 65-116, 1966. https://doi.org/10.21236/AD0646610

[13] Hassani, F. P., Scoble, M. J., Whittaker, B. N. "Application of the point load index test to strength determination of rock and proposals for a new size-correction chart", In: Summers, D. A. (ed.) Rock Mechanics: A State of the Art: Proceedings of the 21st U.S. Symposium on Rock Mechanics, University of Missouri, Rolla, MO, USA, 1980, pp. 543–565.

[14] Read, J. R. L., Thornten, P. N., Regan, W. M. "A rational approach to the point load test", In: Third Australian-New Zealand Conference on Geomechanics, Institution of Professional Engineers New Zealand, Wellington, New Zealand, 1980, 2-35-2-39.

[15] Singh, D. P. "Determination of some engineering properties of weak rocks", In: Proceedings of the International Symposium on Weak Rock, Tokyo, Japan, 1981, vol. 1, pp. 21–24. ISBN 9789061912064

[16] Gunsallus, K. L., Kulhawy, F. H. "A comparative evaluation of rock strength measures", International Journal of Rock Mechanics and Mining Sciences & Geomechanical Abstracts, 21(5), pp. 233–248, 1984. https://doi.org/10.1016/0148-9062(84)92680-9

[17] Das, B. M. "Evaluation of the point load strength for soft rock classification", In: Proceedings of the 4th International Conference on Ground Control in Mining, Morgantown, WV, USA, 1985, pp. 220–226.

[18] Hawkins, A. B., Olver, J. A. G. "Point load tests: Correlation factor and contractual use. An example from the Corallian at Weymouth", Geological Society, London, Engineering Geology Special Publications, 2(1), pp. 269–271, 1986. https://doi.org/10.1144/GSL.1986.002.01.48

[19] O'Rourke, J. E. "Rock index properties for geoengineering in underground development", Mining Engineering, 41(2), pp. 106–109, 1989.

[20] Vallejo, L. E., Welsh Jr., R. A., Robinson, M. K. "Correlation between unconfined compressive and point load strength for Appalachian rocks", In: Khair, A. W. (ed.) Rock Mechanics as a Guide for Efficient Utilization of Natural Resources: Proceeding of the 30th U.S. Symposium, A.A. Balkema, Rotterdam, The Netherlands, 1989 pp. 465–468. ISBN 9061918715

[21] Cargill, J. S., Shakoor, A. "Evaluation of empirical methods for measuring the uniaxial compressive strength of rock", International Journal of Rock Mechanics and Mining Sciences & Geomechanics Abstracts, 27(6), pp. 495–503, 1990. https://doi.org/10.1016/0148-9062(90)91001-N

[22] Tsidzi, K. E. N. "Point load-uniaxial compressive strength correlation", In: Wittke W. (ed.) Proceedings of the 7th ISRM Congress, A.A. Balkema, Rotterdam, The Netherlands, 1, 1991, pp. 637–639. ISBN 9789054100133

[23] Ghosh, D. K., Srivastava, M. "Point-load strength: An index for classification of rock material", Bulletin of the International Association of Engineering Geology, 44, pp. 27–33, 1991. https://doi.org/10.1007/BF02602707

[24] Grasso, P., Xu, S., Mahtab, A. "Problems and promises of index testing of rocks", In: Tillerson, J. R., Wawersik, W. R. (eds.) Proceedings of the 33rd U.S. Symposium on Rock Mechanics, A.A. Balkema, Rotterdam, The Netherlands, 1992, pp. 879–888. ISBN 9789054100454

[25] Singh, V. K., Singh, D. P. "Correlation between point load index and compressive strength for quartzite rocks", Geotechnical & Geological Engineering, 11(4), pp. 269–272, 1993. https://doi.org/10.1007/BF00466369

[26] Ulusay, R., Türeli, K., Ider, M. H. "Prediction of Engineering Properties of a selected Litharenite Sandstone from its Petrographic Characteristics using Correlation and Multivariate Statistical Techniques", Engineering Geology, 38(1–2), pp. 135–157,1994. https://doi.org/10.1016/0013-7952(94)90029-9

[27] Chau, K. T., Wong, R. H. C. "Uniaxial compressive strength and point load strength of rocks", International Journal of Rock Mechanics and Mining Sciences & Geomechanical Abstracts, 33(2), pp. 183–188, 1996. https://doi.org/10.1016/0148-9062(95)00056-9

[28] Smith, H. J. "The point load test for weak rock in dredging applications", International Journal of Rock Mechanics and Mining Sciences, 34(3–4), 295, 304, 1997. https://doi.org/10.1016/S1365-1609(97)00063-4

[29] Rusnak, J., Mark, C. "Using the point load test to determine the uniaxial compressive strength of coal measure rock", In: Peng, S. S., Mark, C. (eds.) Proceedings of the 19th International Conference on Ground Control in Mining, Morgantown, WV, USA, 2000, pp. 362–371.

[30] Tuğrul, A., Zarif, I. H. "Correlation of mineralogical and textural characteristics with engineering properties of selected granitic rocks from Turkey", Engineering Geology, 51(4), pp. 303–317,1999. https://doi.org/10.1016/S0013-7952(98)00071-4

[31] Kahraman, S. "Evaluation of simple methods for assessing the uniaxial compressive strength of rock", International Journal of Rock Mechanics and Mining Sciences, 38(7), pp. 981–994, 2001. https://doi.org/10.1016/S1365-1609(01)00039-9

[32] Sulukcu, S., Ulusay, R. "Evaluation of the Block Punch Index Test with particular reference to the Size effect, Failure Mechanism and its Effectiveness in Predicting Rock Strength", International Journal of Rock Mechanics and Mining Sciences, 38(8), pp. 1091–1111, 2001. https://doi.org/10.1016/S1365-1609(01)00079-X

[33] Quane, S. L., Russel, J. K. "Rock strength as a metric of welding intensity in pyroclastic deposits", European Journal of Mineralogy, 15(5), pp. 855–864, 2003. https://doi.org/10.1127/0935-1221/2003/0015-0855

[34] Tsiambaos, G., Sabatakakis, N. "Considerations on strength of intact sedimentary rocks", Engineering Geology, 72(3–4), pp. 261–273, 2004. https://doi.org/10.1016/j.enggeo.2003.10.001

[35] Fener, M., Kahraman, S., Bilgil, A., Gunaydin, O. "A comparative evaluation of indirect methods to estimate the compressive strength of rocks", Rock Mechanics and Rock Engineering, 38(4), pp. 329–343, 2005. https://doi.org/10.1007/s00603-005-0061-8

[36] Kahraman, S., Gunaydin, O., Fener, M. "The effect of porosity on the relation between uniaxial compressive strength and point load index", International Journal of Rock Mechanics and Mining Sciences, 42(4), pp. 584–589, 2005. https://doi.org/10.1016/j.ijrmms.2005.02.004

[37] Agustawijaya, D. S. "The uniaxial compressive strength of soft rock", Civil Engineering Dimension, 9(1), pp. 9–14, 2007. https://doi.org/10.9744/ced.9.1.pp.%209-14

[38] Yılmaz, I., Yuksek, A. G. "An example of artificial neural network (ANN) application for indirect estimation of rock parameters", Rock Mechanics and Rock Engineering, 41(5), pp. 781–795, 2008. https://doi.org/10.1007/s00603-007-0138-7

[39] Diamantis, K., Gartzos, E., Migiros, G. "Study on uniaxial compressive strength, point load strength index, dynamic and physical properties of serpentinites from central Creece: Test results and empirical relations", Engineering Geology, 108(3–4), pp. 199–207, 2009. https://doi.org/10.1016/j.enggeo.2009.07.002

[40] Sabatakakis, N., Koukis, G., Tsiambaos, G., Papanakli, S. "Index properties and strength variation controlled by microstructure for sedimentary rocks", Engineering Geology, 97(1–2), pp. 80–90, 2009. https://doi.org/10.1016/j.enggeo.2007.12.004

[41] Kahraman, S., Gunaydin, O. "The effect of rock classes on the relation between uniaxial compressive strength and point load index", Bulletin of Engineering Geology and the Environment, 68(3), pp. 345–353, 2009. https://doi.org/10.1007/s10064-009-0195-0

[42] Basu, A., Kamran, M. "Point load test on schistose rocks and its applicability in predicting uniaxial compressive strength", International Journal of Rock Mechanics and Mining Sciences, 47(5), pp. 823–828, 2010. https://doi.org/10.1016/j.ijrmms.2010.04.006

[43] Tahir, M., Mohammad, N., Din, F. "Strength parameters and their inter-relationship for limestone of Cherat and Kohat areas of Khyber Pakhtunkhwa", Journal of Himalayan Earth Sciences, 44(2), pp. 45–51, 2011.

[44] Heidari, M., Khanlari, G., Torabi Kaveh, M., Kargarian, S." Predicting the uniaxial compressive and tensile strengths of gypsum rock by point load testing", Rock Mechanics and Rock Engineering, 45(2), pp. 265–273, 2012. https://doi.org/10.1007/s00603-011-0196-8

[45] Karaman, K., Kesimal, A. "Kayaçların tek eksenli basınç dayanımı tahmininde nokta yükü deney yöntemleri ve porozitenin değerlendirilmesi" (Point load test methods and evaluation of porosity in estimating the uniaxial compressive strength of rocks), Scientific Mining Journal, 51(4), pp. 3–14, 2012. (in Turkish)

[46] Kohno, M., Maeda, H. "Relationship between point load strength index and uniaxial compressive strength of hydrothermally altered soft rocks", International Journal of Rock Mechanics and Mining Sciences, 50, pp. 147–157, 2012. https://doi.org/10.1016/j.ijrmms.2012.01.011

[47] Basu, A. "Mechanical characterization of schistose rocks", In: The ISRM International Symposium – EUROCK 2012, Stockholm, Sweden, 2012, ISRM-EUROCK-2012-025.

[48] Singh, T. N., Kainthola, A., Venkatesh, A. "Correlation between point load index and uniaxial compressive strength for different rock types", Rock Mechanics and Rock Engineering, 45(2), pp. 259–264.2012. https://doi.org/10.1007/s00603-011-0192-z

[49] Mishra, D. A., Basu, A. "Estimation of uniaxial compressive strength of rock materials by index tests using regression analysis and fuzzy inference system", Engineering Geology, 160, pp. 54–68, 2013. https://doi.org/10.1016/j.enggeo.2013.04.004

[50] Li, D., Wong, L. N. Y. "Point load test on meta-sedimentary rocks and correlation to UCS and BTS", Rock Mechanics and Rock Engineering, 46(4), pp. 889–896, 2013. https://doi.org/10.1007/s00603-012-0299-x

[51] Tandon, R. S., Gupta, V. "The control of mineral constituents and textural characteristics on the petrophysical & mechanical (PM) properties of different rocks of the Himalaya", Engineering Geology, 153, pp. 125–143, 2013. https://doi.org/10.1016/j.enggeo.2012.11.005

[52] Kahraman, S. "The determination of uniaxial compressive strength from point load strength for pyroclastic rock", Engineering Geology, 170, pp. 33–42, 2014. https://doi.org/10.1016/j.enggeo.2013.12.009

[53] Momeni, E., Nazir, R., Armaghani, D. J., Amin, M. F. M., Mohamad, E. T. "Predication of unconfined compressive strength of rocks: A review paper", Jurnal Teknologi (Sciences & Engineering), 77(11), pp. 43–50, 2015. https://doi.org/10.11113/jt.v77.6393

[54] Lindqvist, J. E., Åkesson, U., Malaga, K. "Microstructure and functional properties of rock materials", Materials Characterization, 58(11–12), pp. 1183–1188, 2007. https://doi.org/10.1016/j.matchar.2007.04.012

[55] Ioanna, I., Dimitrios, R., Theodora, P., Paris, T. "Geotechnical and mineralogical properties of weak rocks from Central Greece", Central European Journal of Geosciences, 1(4), pp. 431–442, 2009. https://doi.org/10.2478/v10085-009-0029-0

[56] Yusof, N. Q. A. M., Zabidi. H. "Correlation of mineralogical and textural characteristics with engineering properties of granitic rock from Hulu Langat, Selangor", Procedia Chemistry, 19, pp. 975–980, 2016. https://doi.org/10.1016/j.proche.2016.03.144

[57] Li, H., Li, H., Wang, K., Liu, C. "Effect of rock composition microstructure and pore characteristics on its rock mechanics properties", International Journal of Mining Science and Technology, 28(2), pp. 303–308, 2018. https://doi.org/10.1016/j.ijmst.2017.12.008

[58] Yasir, S. F., Awang, H., Ayub, M. I. H. "The relationship of sandstone's strength with mineral content and petrographic characteristics in Sungai Tekai, Jerantut, Pahang", AIP Conference Proceedings, 2020(1), 020010, 2018. https://doi.org/10.1063/1.5062636

[59] Davarpanah, S. M., Sharghi, M., Tarifard, A., Török, Á., Vásárhelyi, B. "Studies on the Mechanical Properties of Dry, Saturated, and Frozen Marls Using Destructive and Non-destructive Laboratory Approaches", Iranian Journal of Science and Technology, Transactions of Civil Engineering, 46(2), pp. 1311–1328, 2022. https://doi.org/10.1007/s40996-021-00690-z

[60] Yaylacı, M., Abanoz, M., Yaylacı, E. U., Ölmez, H., Sekban, D. M., Birinci, A. "Evaluation of the contact problem of functionally graded layer resting on rigid foundation pressed via rigid punch by analytical and numerical (FEM and MLP) methods", Archive of Applied Mechanics, 92(6), pp. 1953–1971, 2022. https://doi.org/10.1007/s00419-022-02159-5

[61] Yaylaci, M., Abanoz, M., Yaylaci, E. U., Ölmez, H., Sekban, D. M., Birinci, A. "The contact problem of the functionally graded layer resting on rigid foundation pressed via rigid punch", Steel and Composite Structures, 43(5), pp. 661–672, 2022. https://doi.org/10.12989/scs.2022.43.5.661

[62] Yaylaci, E. U., Öner, E., Yaylaci, M., Özdemir, M. E., Abushattal, A., Birinci, A. "Application of artificial neural networks in the analysis of the continuous contact problem", Structural Engineering and Mechanics, 84(1), pp. 35–48, 2022. https://doi.org/10.12989/sem.2022.84.1.035

[63] Yaylaci, M., Yaylacı, E.U., Özdemir, M. E., Ay, S., Özturk, Ş. "Implementation of finite element and artificial neural network methods to analyze the contact problem of a functionally graded layer containing crack", Steel and Composite Structures, 45(4), pp. 501–511, 2022. https://doi.org/10.12989/scs.2022.45.4.501

[64] Yaylaci, M. "The investigation crack problem through numerical analysis", Structural Engineering and Mechanics, 57(6), pp. 1143–1156, 2016. https://doi.org/10.12989/sem.2016.57.6.1143

[65] Yaylaci, M., Yaylacı, E. U., Özdemir, M. E., Öztürk, Ş., Sesli, H. "Vibration and buckling analyses of FGM beam with edge crack: Finite element and multilayer perceptron methods", Steel and Composite Structures, 46(4), pp. 565–575, 2023. https://doi.org/10.12989/scs.2023.46.4.565

[66] Mehrgini, B., Memarian, H., Dusseault, M. B., Ghavidel, A., Heidarizadeh, M. "Geomechanical characteristics of common reservoir caprock in Iran (Gachsaran Formation), experimental and statistical analysis", Journal of Natural Gas Science and Engineering, 34, pp. 898–907, 2016. https://doi.org/10.1016/j.jngse.2016.07.058

[67] Kelly, J. R., Wakeley, L. D., Broadfoot, S. W., "Geologic setting of Mosul dam and its engineering implications", KIP Articles, 2294, 2007.

[68] Sissakian, V. K., Al-Ansari, N., Knutsson, S. "Karstification Effect on the Stability of Mosul Dam and Its Assessment, North Iraq", Engineering, 6(2), pp. 84–92, 2014. https://doi.org/10.4236/eng.2014.62012

[69] Adamo, N., Al-Ansari, N. "Mosul dam the full story: Engineering Problems", Journal of Earth Sciences and Geotechnical Engineering, 6(3), pp. 213–244, 2016.

[70] Al-Ansari, N. A., Adamo, N., Sissakian, V., Knutsson, S., Laue, J. "Is Mosul Dam the Most Dangerous Dam in the World? Review of Previous Work and Possible Solutions", Engineering, 9(10), pp. 801–823, 2017. https://doi.org/10.4236/eng.2017.910048

[71] Rahimi, M. R., Mohammadi, S. D., Heidari, M., Jalali, S. H. "Evaluation of the needle penetration test to estimate the uniaxial compressive strength of gypsum rocks", Arabian Journal of Geosciences, 13(1), 14, 2020. https://doi.org/10.1007/s12517-019-4989-5

[72] ASTM "ASTM D7012-23 Standard Test Methods for Compressive Strength and Elastic Moduli of Intact Rock Core Specimens under Varying States of Stress and Temperatures", ASTM International, West Conshohocken, PA, USA, 2023. https://doi.org/10.1520/D7012-23

[73] Bieniawski, Z. T., Bernede, M. J. "Suggested methods for determining the uniaxial compressive strength and deformability of rock materials: Part 1. Suggested method for determining deformability of rock materials in uniaxial compression", International Journal of Rock Mechanics and Mining Sciences & Geomechanics Abstracts, 16(2), pp. 135–140, 1979. https://doi.org/10.1016/0148-9062(79)91451-7

[74] ASTM "ASTM D4543-19 Standard Practices for Preparing Rock Core as Cylindrical Test Specimens and Verifying Conformance to Dimensional and Shape Tolerances", ASTM International, West Conshohocken, PA, USA, 2019. https://doi.org/10.1520/D4543-19

[75] Rahimi, M. R., Mohammadi, S. D., Beydokhti, A. T. "Correlation between Schmidt hammer hardness, strength properties and mineral compositions of sulfate rocks", Geotechnical and Geological Engineering, 40(2), pp. 545–574, 2022. https://doi.org/10.1007/s10706-021-01878-w

[76] Rahimi, M. R., Mohammadi, S. D., Beydokhti, A. T. "Effects of mineral composition and texture on durability of sulfate rocks in Gachsaran Formation, Iran", Geotechnical and Geological Engineering, 38(3), pp. 2619–2637, 2020. https://doi.org/10.1007/s10706-019-01173-9

[77] Mohammadi S. D., Rahimi, M. R., Taleb Bydokhti, A. "Saturation Procedures of Soluble Rocks (Emphasizing on Gypsum-Anhydrite Rocks)", Scientific Quarterly Journal of Iranian Association of Engineering Geology, 13(3), pp. 97–111, 2020. [online] Available at: http://www.jiraeg.ir/article_113119.html

[78] Rahimi, M. R., Mohammadi, S. D., Beydokhti, A. T. "Correlation between the mineral composition and strength properties of sulfate rocks", Quarterly Journal of Engineering Geology and Hydrology, 55(2), qjegh2020-173, 2022. https://doi.org/10.1144/qjegh2020-173

[79] Bell, F. G. "A survey of the engineering properties of some anhydrite and gypsum from the north and midlands of England", Engineering Geology, 38(1–2), pp. 1–23, 1994. https://doi.org/10.1016/0013-7952(94)90021-3

[80] Karacan, E., Yilmaz, I. "Geotechnical evaluation of Miocene gypsum from Sivas (Turkey)", Geotechnical and Geological Engineering, 18(2), pp. 79–90, 2000. https://doi.org/10.1023/A:1008969726200

[81] Rahimi, M. R., Mohammadi, S. D., Heidari, M., Jalali, S. H. "Correlation between mineral composition and P-wave velocity, strength and textural properties of sulfate rocks in dry and saturated conditions", Journal of Applied Geophysics, 192, 104397, 2021. https://doi.org/10.1016/j.jappgeo.2021.104397

Appendix A

Table A1 The results of UCTs, APLTs, DPLTs for 182 series of rock samples in oven dried conditions

Row	Sample NO	L (mm)	d (mm)	L/d	ρ_{dry} g/cm^3	$UCS_{(Dry)}$ (MPa)	$I_{s(50)(Axial)(Dry)}$ (MPa)	$I_{s(50)(Diametral)(Dry)}$ (MPa)	Mineral composition			Texture
									GP	AN	CMs	
1	KA1-2-1	134.60	54.55	2.47	2.32	27.79	2.12	1.87	75.83	0.00	24.17	Alabaster
2	KA1-2-2	133.50	54.70	2.44	2.31	23.92	1.30	1.28	75.83	0.00	24.17	Alabaster
3	KA1-2-3	132.80	54.61	2.43	2.30	28.07	2.14	1.90	75.83	0.00	24.17	Alabaster
4	KA1-2-6	133.95	54.56	2.46	2.31	25.62	1.45	1.41	75.83	0.00	24.17	Alabaster
5	KA1-2-8	134.81	54.63	2.47	2.31	27.51	1.77	1.73	75.83	0.00	24.17	Alabaster
6	KA1-3-1	130.77	52.38	2.50	2.31	22.89	0.96	1.05	60.96	3.64	35.39	Alabaster
7	KA1-3-2	130.56	52.39	2.49	2.30	33.16	2.24	2.23	60.96	3.64	35.39	Alabaster
8	KA1-3-14	131.43	52.86	2.49	2.31	39.70	2.39	2.65	60.96	3.64	35.39	Alabaster
9	KA1-3-17	131.78	52.72	2.50	2.30	37.56	2.34	2.56	60.96	3.64	35.39	Alabaster
10	KA1-3-21	130.99	52.73	2.48	2.32	32.74	2.23	2.11	60.96	3.64	35.39	Alabaster
11	KA1-5-1	133.86	54.24	2.47	2.32	23.33	1.25	1.07	60.96	3.64	35.39	Alabaster
12	KA1-5-2	133.97	54.26	2.47	2.31	24.95	1.40	1.35	60.96	3.64	35.39	Alabaster
13	KA1-6-1	134.63	53.97	2.49	2.30	20.38	0.72	0.86	75.83	0.00	24.17	Alabaster
14	KA1-6-2	133.47	54.06	2.47	2.29	27.26	1.75	1.61	75.83	0.00	24.17	Alabaster
15	KA1-6-3	135.32	53.97	2.51	2.30	25.93	1.62	1.48	75.83	0.00	24.17	Alabaster
16	KA4-1-2	135.8	52.78	2.57	2.29	13.61	0.22	0.34	87.31	2.32	10.37	Porphyry
17	KA4-1-3	135.02	52.77	2.56	2.33	25.95	1.16	1.42	87.31	2.32	10.37	Porphyry
18	KA4-1-4	135.31	52.78	2.56	2.31	20.45	0.86	1.08	87.31	2.32	10.37	Porphyry
19	KA4-2-1	124.85	52.01	2.40	2.28	19.47	0.64	0.85	87.31	2.32	10.37	Porphyry
20	KA4-2-3	127.18	52.03	2.44	2.27	15.70	0.24	0.39	87.31	2.32	10.37	Porphyry
21	KA4-5-2	136.6	53.97	2.53	2.34	22.11	0.92	1.15	87.31	2.32	10.37	Porphyry
22	KA4-5-7	134.66	54.2	2.48	2.31	17.35	0.55	0.69	87.31	2.32	10.37	Porphyry
23	KA4-5-9	133.62	54.32	2.46	2.33	20.34	0.67	0.97	87.31	2.32	10.37	Porphyry
24	KA4-5-13	134.28	54.27	2.47	2.30	16.04	0.47	0.44	87.31	2.32	10.37	Porphyry
25	KA4-5-14	134.65	54.25	2.48	2.30	16.54	0.52	0.54	87.31	2.32	10.37	Porphyry
26	KG7-1-1	133.74	52.66	2.54	2.26	23.36	1.55	1.84	91.79	1.72	6.49	Porphyry
27	KG7-1-2	133.99	52.3	2.56	2.23	17.97	0.90	0.73	91.79	1.72	6.49	Porphyry
28	KG7-1-3	133.67	52.25	2.56	2.24	30.17	2.23	2.80	91.79	1.72	6.49	Porphyry
29	KG7-3-1	132.46	52.24	2.54	2.27	23.32	1.50	1.51	91.79	1.72	6.49	Porphyry
30	KG7-3-2	132.33	52.36	2.53	2.26	36.65	2.49	3.37	91.79	1.72	6.49	Porphyry
31	KG7-3-3	133.35	52.29	2.55	2.26	27.87	1.93	2.51	91.79	1.72	6.49	Porphyry
32	KG7-3-4	132.36	52.32	2.53	0.00	23.94	1.81	2.25	91.79	1.72	6.49	Porphyry
33	KG7-3-5	132.52	52.37	2.53	2.26	23.90	1.68	1.95	91.79	1.72	6.49	Porphyry
34	KG7-4-2	132.84	54.31	2.45	2.29	28.18	2.05	2.62	90.22	1.31	8.47	Porphyry
35	KG7-4-3	135.64	54.31	2.50	2.27	28.29	2.12	2.71	90.22	1.31	8.47	Porphyry

Table A1 The results of UCTs, APLTs, DPLTs for 182 series of rock samples in oven dried conditions (continued)

Row	Sample NO	L (mm)	d (mm)	L/d	ρ_{dry} g/cm^3	$UCS_{(Dry)}$ (MPa)	$I_{s(50)(Axial)(Dry)}$ (MPa)	$I_{s(50)(Diametral)(Dry)}$ (MPa)	Mineral composition			Texture
									GP	AN	CMs	
36	KG7-4-4	134.46	54.23	2.48	2.30	35.58	2.41	3.11	90.22	1.31	8.47	Porphyry
37	KG7-6-1	134.16	54.07	2.48	2.22	21.10	0.93	1.27	91.00	1.52	7.48	Porphyry
38	KG7-6-3	133.69	54.04	2.47	2.21	22.47	1.42	1.28	91.00	1.52	7.48	Porphyry
39	KG9-1-1	130.84	52.71	2.48	2.27	40.60	2.43	2.58	69.09	0.00	30.91	Porphyry
40	KG9-1-2	131.43	52.55	2.50	2.27	34.16	2.29	1.88	69.09	0.00	30.91	Porphyry
41	KG9-1-3	132.87	52.64	2.52	2.28	31.69	2.21	1.76	69.09	0.00	30.91	Porphyry
42	KG9-1-4	132.48	52.64	2.52	2.28	39.67	2.34	2.34	69.09	0.00	30.91	Porphyry
43	KG9-1-8	132.23	52.68	2.51	2.27	42.77	2.49	2.92	69.09	0.00	30.91	Porphyry
44	KG9-1-9	131.82	52.74	2.50	2.27	41.56	2.46	2.82	69.09	0.00	30.91	Porphyry
45	KG9-2-1	132.64	54.93	2.41	2.65	45.56	3.09	2.85	18.95	72.91	8.15	Porphyry
46	KG9-2-2	131.71	54.94	2.40	2.64	21.40	1.63	1.51	18.95	72.91	8.15	Porphyry
47	KG9-2-4	132.04	54.91	2.40	2.66	23.66	2.05	1.58	18.95	72.91	8.15	Porphyry
48	KG9-2-6	131.47	54.86	2.40	2.65	46.41	3.26	3.19	18.95	72.91	8.15	Porphyry
49	KG9-5-4	134.16	53.96	2.49	2.27	26.78	1.90	1.21	72.96	1.15	25.89	Porphyry
50	KG9-5-8	134.42	53.74	2.50	2.27	28.65	2.10	1.49	72.96	1.15	25.89	Porphyry
51	KG9-5-9	134.79	53.92	2.50	2.27	25.39	1.73	1.12	72.96	1.15	25.89	Porphyry
52	KG10-3-1	135.59	53.63	2.53	2.63	31.14	2.36	2.10	20.86	76.32	2.82	Porphyry
53	KG10-3-3	135.03	54.02	2.50	2.66	26.13	2.16	1.77	20.86	76.32	2.82	Porphyry
54	KG10-3-4	134.68	54.04	2.49	2.64	33.96	2.45	2.21	20.86	76.32	2.82	Porphyry
55	KG10-3-6	135.30	53.63	2.52	2.65	28.37	2.30	1.91	20.86	76.32	2.82	Porphyry
56	KG10-3-7	136.05	53.63	2.54	2.64	41.39	2.96	2.73	20.86	76.32	2.82	Porphyry
57	KG10-3-8	135.19	53.63	2.52	2.62	35.49	2.47	2.29	20.86	76.32	2.82	Porphyry
58	KG10-3-9	134.35	53.62	2.51	2.64	32.01	2.43	2.16	20.86	76.32	2.82	Porphyry
59	KG10-3-10	135.87	53.63	2.53	2.64	36.28	2.86	2.35	20.86	76.32	2.82	Porphyry
60	KG10-3-11	135.92	53.61	2.54	2.65	36.46	2.90	2.50	20.86	76.32	2.82	Porphyry
61	KG13-2-1	132.09	52.10	2.54	2.30	56.34	2.34	3.54	48.74	21.02	30.23	Porphyry
62	KG13-2-2	128.50	52.12	2.47	2.36	69.86	2.65	3.96	48.74	21.02	30.23	Porphyry
63	KG13-2-3	131.58	52.12	2.52	2.25	29.67	1.70	1.60	48.74	21.02	30.23	Porphyry
64	KG13-2-4	131.46	52.02	2.53	2.26	39.43	2.26	2.46	48.74	21.02	30.23	Porphyry
65	KG13-2-8	131.52	52.34	2.51	2.45	36.12	2.06	1.85	48.74	21.02	30.23	Porphyry
66	KG13-2-9	132.61	52.51	2.53	2.36	33.42	1.88	1.78	48.74	21.02	30.23	Porphyry
67	KG13-5-3	132.24	54.23	2.44	2.69	26.47	1.63	1.11	39.90	55.11	4.99	Porphyry
68	KG13-5-4	132.24	54.23	2.44	2.71	38.82	2.25	2.31	39.90	55.11	4.99	Porphyry
69	KG13-5-8	134.15	54.22	2.47	2.28	37.46	2.09	2.11	39.90	55.11	4.99	Porphyry
70	KG13-6-1	135.45	54.21	2.50	2.27	42.99	2.32	2.79	69.98	1.24	28.78	Porphyry
71	KG13-6-2	135.69	54.10	2.51	2.22	24.49	1.32	0.84	69.98	1.24	28.78	Porphyry
72	MG4-1-1	132.33	52.24	2.53	2.64	43.43	2.46	1.98	53.71	46.59	0.00	Porphyry
73	MG4-6-1	136.01	52.59	2.59	2.54	54.09	2.77	2.13	54.62	43.82	1.56	Porphyry
74	MG4-6-2	136.35	52.59	2.59	2.49	62.32	3.61	2.64	54.62	43.82	1.56	Porphyry
75	MG4-8-1	135.43	52.64	2.57	2.70	49.32	2.58	2.10	67.61	29.98	2.42	Porphyry
76	MG4-8-2	136.46	52.62	2.59	2.71	64.90	3.62	2.75	67.61	29.98	2.42	Porphyry
77	MG4-8-7	136.53	52.66	2.59	2.56	69.47	3.95	2.97	67.61	29.98	2.42	Porphyry
78	MG4-8-8	136.41	52.83	2.58	2.55	58.76	3.21	2.41	54.62	43.82	1.56	Porphyry
79	MG4-8-9	135.79	52.49	2.59	2.58	54.28	2.99	2.14	54.62	43.82	1.56	Porphyry
80	MG5-10-1	134.27	54.50	2.46	2.58	44.64	2.82	3.74	39.81	60.19	0.00	Porphyry

Table A1 The results of UCTs, APLTs, DPLTs for 182 series of rock samples in oven dried conditions (continued)

Row	Sample NO	L (mm)	d (mm)	L/d	ρ_{dry} g/cm^3	$UCS_{(Dry)}$ (MPa)	$I_{s(50)(Axial)(Dry)}$ (MPa)	$I_{s(50)(Diametral)(Dry)}$ (MPa)	Mineral composition			Texture
									GP	AN	CMs	
81	MG5-3-1	135.46	52.61	2.57	2.47	28.34	2.67	2.80	70.22	24.26	5.52	Porphyry
82	MG5-4-1	134.77	52.63	2.56	2.16	18.49	1.61	1.19	89.07	8.51	2.42	Porphyry
83	MG5-4-2	134.46	52.61	2.56	2.15	12.76	1.29	0.91	89.07	8.51	2.42	Porphyry
84	MG5-4-3	134.35	52.64	2.55	2.21	27.96	2.58	2.70	89.07	8.51	2.42	Porphyry
85	MG5-4-4	133.95	52.64	2.54	2.19	18.78	1.87	1.62	89.07	8.51	2.42	Porphyry
86	MG5-4-7	133.68	52.43	2.55	2.18	21.51	1.96	2.06	89.07	8.51	2.42	Porphyry
87	MG5-4-8	134.49	52.73	2.55	2.20	25.67	2.57	2.63	89.07	8.51	2.42	Porphyry
88	MG5-6-1	135.96	52.65	2.58	2.57	22.92	1.68	1.89	26.56	70.77	2.66	Porphyry
90	MG5-6-2	135.86	52.63	2.58	2.58	35.51	2.37	3.04	26.56	70.77	2.66	Porphyry
91	MG5-6-3	137.53	52.63	2.61	2.61	27.98	1.95	2.67	26.56	70.77	2.66	Porphyry
92	MG5-6-4	135.83	52.65	2.58	2.58	25.38	1.90	2.45	26.56	70.77	2.66	Porphyry
93	MG5-6-5	134.93	52.77	2.56	2.56	32.08	2.10	2.71	26.56	70.77	2.66	Porphyry
94	MG5-6-8	135.78	52.76	2.57	2.57	18.62	1.39	1.68	26.56	70.77	2.66	Porphyry
89	MG5-6-10	135.49	52.82	2.57	2.52	33.93	2.17	2.81	26.56	70.77	2.66	Porphyry
95	MG5-7-5	136.09	52.69	2.58	2.58	56.88	3.18	4.23	26.56	70.77	2.66	Porphyry
96	MG5-8-3	135.12	53.72	2.52	2.52	36.11	2.64	3.09	39.81	60.19	0.00	Porphyry
97	MG5-8-5	135.66	53.59	2.53	2.53	48.97	2.86	3.84	39.81	60.19	0.00	Porphyry
98	MG5-9-1	135.85	53.82	2.52	2.52	40.10	2.68	3.54	26.56	70.77	2.66	Porphyry
99	MG6-5-A2	140.07	52.60	2.66	2.35	28.29	2.52	2.26	12.59	87.41	0.00	Porphyry
100	MG6-5-A3	137.25	52.64	2.61	2.61	31.30	2.74	2.49	12.59	87.41	0.00	Porphyry
101	MG6-5-B1	139.05	52.61	2.64	2.64	29.13	2.63	2.46	12.59	87.41	0.00	Porphyry
102	MG6-5-B2	135.76	52.70	2.58	2.58	36.57	3.12	3.07	12.59	87.41	0.00	Porphyry
103	MG6-5-B3	136.29	52.68	2.59	2.59	31.91	2.81	2.59	12.59	87.41	0.00	Porphyry
104	MG6-7-1	134.98	53.77	2.51	2.56	34.17	3.01	2.96	23.12	76.88	0.00	Porphyry
107	MG6-7-2	135.67	53.81	2.52	2.62	42.32	3.39	3.37	23.12	76.88	0.00	Porphyry
108	MG6-7-3	134.71	53.81	2.50	2.73	47.79	3.54	3.48	23.12	76.88	0.00	Porphyry
109	MG6-7-4	128.64	53.79	2.39	2.73	20.38	2.16	1.91	23.12	76.88	0.00	Porphyry
110	MG6-7-9	135.38	53.80	2.52	2.63	36.86	3.22	3.11	23.12	76.88	0.00	Porphyry
105	MG6-7-11	134.69	53.68	2.51	2.68	49.65	4.18	3.75	23.12	76.88	0.00	Porphyry
106	MG6-7-12	134.92	53.59	2.52	2.48	27.31	2.50	2.14	23.12	76.88	0.00	Porphyry
111	MG11-1A-1	135.26	53.84	2.51	2.71	56.35	2.88	3.35	27.48	70.78	1.74	Porphyry
112	MG11-1A-4	135.26	53.84	2.51	2.71	61.67	3.25	3.95	27.48	70.78	1.74	Porphyry
113	MG11-2-2	135.99	53.86	2.52	2.71	57.66	3.64	4.52	27.48	70.78	1.74	Porphyry
114	MG11-2-5	135.95	53.83	2.53	2.73	46.83	2.71	2.98	27.48	70.78	1.74	Porphyry
115	MG11-2-6	135.82	53.75	2.53	2.58	54.16	3.45	3.71	27.48	70.78	1.74	Porphyry
116	MG11-2-8	136.27	53.71	2.54	2.59	53.89	3.39	3.48	27.48	70.78	1.74	Porphyry
117	MG11-4-2	135.75	54.04	2.51	2.74	76.16	3.71	4.68	55.07	44.51	0.42	Porphyry
118	MG11-4-5	135.29	54.39	2.49	2.62	71.29	3.52	4.24	55.07	44.51	0.42	Porphyry
119	MG11-4-8	135.67	54.67	2.48	2.65	65.76	3.44	4.17	55.07	44.51	0.42	Porphyry
120	MG11-5-3	130.77	55.17	2.37	2.78	66.97	3.83	4.63	27.48	70.78	1.74	Porphyry
121	MG11-5-4	130.67	55.20	2.37	2.67	49.98	3.23	3.27	27.48	70.78	1.74	Porphyry
122	MG11-6-1	135.26	54.22	2.49	2.69	40.03	2.01	2.19	55.07	44.51	0.42	Porphyry
123	MG11-7-1	135.05	53.12	2.54	2.61	38.08	2.48	2.63	33.82	64.32	1.86	Porphyry
124	MG11-7-2	134.66	53.08	2.54	2.72	49.71	3.03	3.13	33.82	64.32	1.86	Porphyry
125	MG11-8-2	132.13	53.20	2.48	2.66	45.14	2.50	2.60	55.07	44.51	0.42	Porphyry

Table A1 The results of UCTs, APLTs, DPLTs for 182 series of rock samples in oven dried conditions (continued)

Row	Sample NO	L (mm)	d (mm)	L/d	ρ_{dry} g/cm^3	$UCS_{(Dry)}$ (MPa)	$I_{s(50)(Axial)(Dry)}$ (MPa)	$I_{s(50)(Diametral)(Dry)}$ (MPa)	Mineral composition			Texture
									GP	AN	CMs	
126	MG11-8-5	133.56	53.06	2.52	2.65	37.35	1.82	1.96	55.07	44.51	0.42	Porphyry
127	MG11-10-1	135.43	53.35	2.54	2.66	49.95	2.73	3.12	53.39	46.61	0.00	Porphyry
128	MG11-10-6	136.07	53.82	2.53	2.63	48.55	2.63	2.94	53.39	46.61	0.00	Porphyry
129	NG3-1-1	135.89	54.48	2.49	2.28	35.08	2.22	1.96	69.36	1.13	29.51	Alabaster
130	NG3-1-2	133.34	54.47	2.45	2.28	34.58	2.17	1.71	69.36	1.13	29.51	Alabaster
133	NG3-2-2	132.13	54.35	2.43	2.28	39.45	2.45	2.07	74.31	15.06	10.63	Alabaster
134	NG3-2-5	135.31	54.18	2.50	2.28	25.68	2.03	1.38	74.31	15.06	10.63	Alabaster
131	NG3-2-10	135.34	54.38	2.49	2.27	30.12	2.14	1.62	74.31	15.06	10.63	Alabaster
132	NG3-2-11	134.37	54.62	2.46	2.27	29.38	2.12	1.48	74.31	15.06	10.63	Alabaster
135	NG3-6-1	133.28	50.36	2.65	2.31	21.20	1.71	1.03	70.58	12.39	17.02	Alabaster
136	NG3-6-7	133.39	51.42	2.59	2.27	19.86	1.56	0.94	70.58	12.39	17.02	Alabaster
137	NG3-7-1	126.43	52.34	2.42	2.29	22.45	1.87	1.18	98.17	0.78	1.04	Alabaster
138	NG3-9-A1	135.81	54.76	2.48	2.28	24.77	2.02	1.29	81.72	1.97	16.31	Alabaster
139	NG5-1-1	135.65	54.21	2.50	2.31	30.40	2.17	2.13	90.42	3.01	6.58	Alabaster
142	NG5-5-3	135.94	54.23	2.51	2.31	17.74	1.01	1.16	42.60	54.03	3.37	Alabaster
143	NG5-5-8	135.94	54.23	2.51	2.28	26.18	2.13	2.09	42.60	54.03	3.37	Alabaster
140	NG5-5-10	133.68	54.49	2.45	2.26	22.12	1.61	1.70	42.60	54.03	3.37	Alabaster
141	NG5-5-11	132.84	54.37	2.44	2.27	19.16	1.28	1.56	42.60	54.03	3.37	Alabaster
144	NG5-6-2	133.37	54.43	2.45	2.27	30.92	2.61	2.31	84.91	0.64	14.45	Alabaster
145	NG5-6-3	134.87	54.39	2.48	2.27	29.23	2.13	1.99	84.91	0.64	14.45	Alabaster
146	NG5-7-3	135.39	54.52	2.48	2.29	14.76	1.04	0.81	88.87	1.86	9.27	Alabaster
147	NG5-9-A3	133.99	54.74	2.45	2.29	27.82	2.36	2.28	38.30	44.82	16.87	Alabaster
148	NG5-9-B1	131.89	54.64	2.41	2.29	23.99	1.82	1.89	47.51	37.10	15.39	Alabaster
149	NG5-9-B4	135.32	54.76	2.47	2.26	18.06	1.17	1.32	47.51	37.10	15.39	Alabaster
150	NG5-9-B7	133.52	54.62	2.44	2.27	22.86	1.78	1.81	47.51	37.10	15.39	Alabaster
151	NG5-10-B3	131.63	54.66	2.41	2.28	25.01	2.03	1.71	90.97	0.00	9.03	Alabaster
152	NG5-10-B4	127.33	54.70	2.33	2.26	15.55	1.59	1.15	90.97	0.00	9.03	Alabaster
153	NG5-10-B6	130.39	54.63	2.39	2.28	22.56	1.84	1.44	90.97	0.00	9.03	Alabaster
154	NG5-10-B7	129.74	54.28	2.39	2.29	24.07	1.90	1.59	90.97	0.00	9.03	Alabaster
155	NG5-10-B8	132.64	54.71	2.42	2.26	18.79	1.77	1.26	90.97	0.00	9.03	Alabaster
156	NG5-10-B9	131.69	54.62	2.41	2.27	20.19	1.82	1.35	90.97	0.00	9.03	Alabaster
157	TG3-1-1	135.45	53.53	2.53	2.24	15.40	1.13	0.98	90.67	0.00	9.33	Alabaster
158	TG3-1-2	135.80	53.52	2.54	2.23	16.63	1.37	1.13	90.67	0.00	9.33	Alabaster
159	TG3-2-1	134.37	53.37	2.52	2.29	15.81	1.22	1.07	98.00	0.00	2.00	Alabaster
160	TG3-3-1	134.59	53.60	2.51	2.27	22.15	1.64	1.34	90.67	0.00	9.33	Alabaster
161	TG3-3-8	134.68	53.49	2.52	2.27	19.43	1.49	1.15	90.67	0.00	9.33	Alabaster
162	TG3-3-2	135.08	53.61	2.52	2.26	12.27	1.01	0.85	90.67	0.00	9.33	Alabaster
163	TG3-3-3	134.90	53.57	2.52	2.26	26.82	1.95	1.66	90.67	0.00	9.33	Alabaster
164	TG3-5-1	135.40	53.61	2.53	2.30	25.47	1.91	1.54	94.00	4.00	2.00	Alabaster
165	TG3-5-2	136.61	53.60	2.55	2.30	28.89	2.01	1.74	94.00	4.00	2.00	Alabaster
166	TG3-5-3	136.47	53.58	2.55	2.30	21.99	1.58	1.23	94.00	4.00	2.00	Alabaster
167	TG3-7-1	129.40	53.42	2.42	2.27	32.90	2.21	2.15	94.66	1.67	3.68	Alabaster
168	TG3-9-1H	135.56	53.70	2.52	2.28	22.78	1.68	1.38	94.66	1.67	3.68	Alabaster
169	TG3-9-2H	134.94	53.54	2.52	2.27	24.25	1.78	1.42	94.66	1.67	3.68	Alabaster
170	TG3-9-6V	135.82	53.69	2.53	2.27	31.95	2.04	1.91	94.66	1.67	3.68	Alabaster

Table A1 The results of UCTs, APLTs, DPLTs for 182 series of rock samples in oven dried conditions (continued)

Row	Sample NO	L (mm)	d (mm)	L/d	ρ_{dry} g/cm^3	$UCS_{(Dry)}$ (MPa)	$I_{s(50)(Axial)(Dry)}$ (MPa)	$I_{s(50)(Diametral)(Dry)}$ (MPa)	Mineral composition			Texture
									GP	AN	CMs	
171	TG4-1-1	134.24	53.5	2.51	2.27	35.74	2.35	1.83	86.41	2.90	10.69	Alabaster
172	TG4-6-1	134.5	53.23	2.53	2.24	27.31	1.88	1.46	97.00	0.00	3.00	Alabaster
173	TG4-7-1	132.64	53.05	2.50	2.22	30.93	2.16	1.78	96.33	1.00	2.67	Alabaster
174	TG4-7-2	133.67	53.05	2.52	2.25	28.19	2.07	1.61	96.33	1.00	2.67	Alabaster
175	TG10-6-1	135.12	54.26	2.49	2.27	20.32	1.61	1.12	96.33	0.00	4.67	Alabaster
176	TG10-7-1	132.08	54.03	2.44	2.28	44.58	2.48	2.09	96.23	0.00	3.77	Alabaster
177	TG10-8-1	131.23	54.05	2.43	2.28	24.74	1.85	1.32	82.01	8.68	9.31	Alabaster
178	TG10-9-1	110.36	53.35	2.07	2.28	15.68	1.42	1.09	87.01	4.68	8.31	Alabaster
179	TG10-10-1	137.38	53.72	2.56	2.29	22.20	1.77	1.31	97.33	0.00	2.67	Alabaster
180	TG10-10-4	135.8	53.62	2.53	2.25	15.49	1.28	1.06	97.33	0.00	2.67	Alabaster
181	TG10-10-6	134.9	53.49	2.52	2.26	13.82	1.13	0.97	97.33	0.00	2.67	Alabaster
182	TG10-10-7	135.5	52.73	2.57	2.23	15.11	1.14	0.98	97.33	0.00	2.67	Alabaster
Mean		133.94	53.51	2.50	2.39	32.18	2.11	2.07	62.43	27.94	9.63	
Max		140.07	55.20	2.66	2.78	76.16	4.18	4.68	98.17	87.41	35.39	
Min		110.36	50.36	2.07	0.00	12.27	0.22	0.34	12.59	0.00	0.00	
St.D		2.80	0.87	0.06	0.25	13.36	0.76	0.91	27.41	31.22	10.47	

Appendix B

Table B1 The results of UCTs, APLTs, DPLTs for 182 series of rock samples in saturated conditions

Row	Sample NO	L (mm)	d (mm)	L/d	$\rho_{(Sat)}$ (g/cm^3)	$UCS_{(Sat)}$ (MPa)	$I_{s(50)(Axial)(Sat)}$ (MPa)	$I_{s(50)(Diametral)(Sat)}$ (MPa)	Mineral composition			Texture
									GP	AN	CMs	
1	KA1-2-7	131.32	54.67	2.40	0.00	17.02	0.79	0.68	75.83	0.00	24.17	Alabaster
2	KA1-2-9	134.37	54.69	2.46	2.32	15.86	0.63	0.57	75.83	0.00	24.17	Alabaster
3	KA1-2-10	132.85	54.69	2.43	2.3	18.22	0.87	0.80	75.83	0.00	24.17	Alabaster
4	KA1-2-11	132.64	54.48	2.43	2.3	17.48	0.83	0.79	75.83	0.00	24.17	Alabaster
5	KA1-2-12	133.12	54.6	2.44	3.31	19.14	0.97	0.87	75.83	0.00	24.17	Alabaster
6	KA1-2-13	131.98	54.42	2.43	2.31	17.4	0.80	0.75	75.83	0.00	24.17	Alabaster
7	KA1-2-14	133.08	54.51	2.44	2.31	16.86	0.74	0.61	75.83	0.00	24.17	Alabaster
8	KA1-2-16	133.28	54.52	2.44	2.31	18.76	0.94	0.86	75.83	0.00	24.17	Alabaster
9	KA1-3-3	130.67	52.81	2.47	2.30	31.43	1.22	1.08	60.96	3.64	35.39	Alabaster
10	KA1-3-4	130.61	52.76	2.48	2.29	20.73	0.97	0.88	60.96	3.64	35.39	Alabaster
11	KA1-3-10	131.34	52.87	2.48	2.32	36.79	1.33	1.23	60.96	3.64	35.39	Alabaster
12	KA1-3-12	131.12	52.78	2.48	2.27	26.29	1.09	0.95	60.96	3.64	35.39	Alabaster
13	KA1-3-19	131.72	52.71	2.50	2.31	28.24	1.15	1.01	60.96	3.64	35.39	Alabaster
14	KA1-3-25	132.22	52.47	2.52	2.28	33.72	1.26	1.13	60.96	3.64	35.39	Alabaster
15	KA1-3-27	131.56	52.48	2.51	2.32	21.36	1.06	0.93	60.96	3.64	35.39	Alabaster
16	KA1-5-13	129.74	52.69	2.46	2.37	9.97	0.42	0.91	87.31	2.32	10.37	Alabaster
17	KA1-5-15	131.48	52.78	2.49	2.38	11.65	0.49	1.25	87.31	2.32	10.37	Alabaster
18	KA4-1-5	134.2	52.78	2.54	2.30	8.39	0.39	0.66	87.31	2.32	10.37	Porphyry
19	KA4-5-1	134.39	54.09	2.48	2.35	4.59	0.28	0.43	87.31	2.32	10.37	Porphyry
20	KA4-5-3	133.96	54.19	2.47	2.36	6.60	0.32	0.47	87.31	2.32	10.37	Porphyry
21	KA4-5-6	134.8	54.04	2.49	2.36	8.23	0.36	0.62	87.31	2.32	10.37	Porphyry
22	KA4-5-10	134.89	54.38	2.48	2.38	5.75	0.29	0.44	87.31	2.32	10.37	Porphyry
23	KA4-5-11	134.29	54.39	2.47	2.39	7.56	0.33	0.62	87.31	2.32	10.37	Porphyry

Table B1 The results of UCTs, APLTs, DPLTs for 182 series of rock samples in saturated conditions (continued)

Row	Sample NO	L (mm)	d (mm)	L/d	$\rho_{(Sat)}$ (g/cm^3)	$UCS_{(Sat)}$ (MPa)	$I_{s(50)(Axial)(Sat)}$ (MPa)	$I_{s(50)(Diametral)(Sat)}$ (MPa)	Mineral composition			Texture
									GP	AN	CMs	
24	KA4-5-13	133.84	54.48	2.46	2.37	3.56	0.16	0.27	87.31	2.32	10.37	Porphyry
25	KA4-5-14	134.28	54.37	2.47	2.38	4.11	0.21	0.34	87.31	2.32	10.37	Porphyry
26	KG7-1-4	135.77	52.15	2.60	2.29	3.94	0.53	0.53	91.79	1.72	6.49	Porphyry
27	KG7-1-5	133.45	52.14	2.56	2.28	7.31	0.68	0.73	91.79	1.72	6.49	Porphyry
28	KG7-1-6	132.68	52.24	2.54	2.28	12.13	0.81	1.11	91.79	1.72	6.49	Porphyry
29	KG7-3-6	132.63	52.32	2.53	2.29	11.39	0.80	0.97	91.79	1.72	6.49	Porphyry
30	KG7-4-5	138.61	54.21	2.56	2.31	14.15	0.99	1.36	90.22	1.31	8.47	Porphyry
31	KG7-4-7	134.67	54.35	2.48	2.31	12.64	0.82	1.17	90.22	1.31	8.47	Porphyry
32	KG7-4-8	134.52	54.39	2.47	2.31	14.98	1.09	1.60	90.22	1.31	8.47	Porphyry
33	KG7-4-9	134.57	54.3	2.48	2.27	11.06	0.81	1.02	90.22	1.31	8.47	Porphyry
34	KG7-4-10	135.14	54.29	2.49	2.29	9.37	0.76	0.88	90.22	1.31	8.47	Porphyry
35	KG7-6-4	134.81	54.52	2.47	2.3	2.56	0.43	0.36	91.79	1.72	6.49	Porphyry
36	KG7-6-5	134.92	54.18	2.49	2.26	6.69	0.63	0.58	91.00	1.52	7.48	Porphyry
37	KG7-6-6	134.37	54.1	2.48	2.26	9.28	0.71	0.87	91.00	1.52	7.48	Porphyry
38	KG7-6-7	135.33	54.1	2.50	2.25	6.99	0.67	0.62	91.00	1.52	7.48	Porphyry
39	KG9-1-5	130.64	52.81	2.47	2.25	20.48	0.77	1.02	69.09	0.00	30.91	Porphyry
40	KG9-1-6	132.84	52.57	2.53	2.26	23.47	0.80	1.14	69.09	0.00	30.91	Porphyry
41	KG9-1-7	134.62	52.62	2.56	2.28	25.42	0.96	1.37	69.09	0.00	30.91	Porphyry
42	KG9-1-10	134.27	52.48	2.56	2.27	24.56	0.89	1.21	69.09	0.00	30.91	Porphyry
43	KG9-1-11	134.80	52.61	2.56	2.29	28.14	1.00	1.58	69.09	0.00	30.91	Porphyry
44	KG9-1-12	133.62	52.81	2.53	2.3	17.45	0.73	0.95	69.09	0.00	30.91	Porphyry
45	KG9-1-13	134.58	52.73	2.55	2.3	16.29	0.66	0.86	71.03	0.57	28.40	Porphyry
46	KG9-2-8	131.05	54.62	2.40	2.66	36.75	2.09	2.39	18.95	72.91	8.15	Porphyry
47	KG9-3-2	131.48	55.01	2.39	2.31	15.89	0.61	0.84	71.03	0.57	28.40	Porphyry
48	KG9-3-5	132.39	54.69	2.42	2.3	13.66	0.52	0.79	71.03	0.57	28.40	Porphyry
49	KG10-1-1	133.91	52.92	2.53	2.67	28.72	1.85	2.01	34.86	62.35	2.79	Porphyry
50	KG10-1-5	133.37	52.83	2.52	2.72	34.55	2.08	2.30	34.86	62.35	2.79	Porphyry
51	KG10-1-7	132.06	52.87	2.50	2.68	21.53	1.62	1.56	34.86	62.35	2.79	Porphyry
52	KG10-1-9	131.97	52.85	2.50	2.64	17.96	1.34	1.25	34.86	62.35	2.79	Porphyry
53	KG10-1-10	133.77	52.78	2.53	2.69	31.74	2.02	2.18	34.86	62.35	2.79	Porphyry
54	KG10-1-11	133.53	52.83	2.53	2.72	22.89	1.68	1.62	34.86	62.35	2.79	Porphyry
55	KG10-1-15	132.22	52.79	2.50	2.70	26.99	1.71	1.89	34.86	62.35	2.79	Porphyry
56	KG10-4-3	131.89	52.62	2.51	2.73	42.95	2.44	2.98	34.31	62.76	2.93	Porphyry
57	KG10-4-9	131.40	52.62	2.50	2.66	42.43	2.32	2.68	34.31	62.76	2.93	Porphyry
58	KG10-4-11	132.85	52.60	2.53	2.72	39.87	2.17	2.59	34.31	62.76	2.93	Porphyry
59	KG10-5-3	130.18	53.14	2.45	2.77	32.24	2.07	2.26	27.30	69.75	2.95	Porphyry
60	KG10-5-4	125.66	53.67	2.34	2.77	30.85	1.95	2.14	27.30	69.75	2.95	Porphyry
61	KG13-2-5	132.40	52.08	2.54	2.28	29.39	2.59	2.29	48.74	21.02	30.23	Porphyry
62	KG13-4-2	133.10	52.36	2.54	2.25	16.82	0.55	1.17	72.56	0.00	27.44	Porphyry
63	KG13-4-4	133.83	52.22	2.56	2.27	18.82	0.55	1.33	72.56	0.00	27.44	Porphyry
64	KG13-4-6	134.17	52.18	2.57	2.25	14.68	0.34	0.79	72.56	0.00	27.44	Porphyry
65	KG13-4-7	134.34	52.18	2.57	2.28	19.85	1.18	1.52	72.56	0.00	27.44	Porphyry
66	KG13-4-8	134.21	52.20	2.57	2.21	19.77	0.74	1.38	72.56	0.00	27.44	Porphyry
67	KG13-4-9	133.76	52.24	2.56	2.22	19.27	0.70	1.34	72.56	0.00	27.44	Porphyry
68	KG13-4-10	134.24	52.32	2.57	2.23	22.70	1.71	1.83	72.56	0.00	27.44	Porphyry

Table B1 The results of UCTs, APLTs, DPLTs for 182 series of rock samples in saturated conditions (continued)

Row	Sample NO	L (mm)	d (mm)	L/d	$\rho_{(Sat)}$ (g/cm^3)	$UCS_{(Sat)}$ (MPa)	$I_{s(50)(Axial)(Sat)}$ (MPa)	$I_{s(50)(Diametral)(Sat)}$ (MPa)	Mineral composition			Texture
									GP	AN	CMs	
69	KG13-4-12	133.45	52.30	2.55	2.23	16.38	0.49	0.81	72.56	0.00	27.44	Porphyry
70	KG13-6-4	134.76	54.17	2.49	2.25	23.71	1.76	2.03	69.98	1.24	28.78	Porphyry
71	KG13-6-5	133.78	54.16	2.47	2.27	26.32	2.30	2.05	69.98	1.24	28.78	Porphyry
72	MG4-1-3	133.93	52.23	2.56	2.69	36.03	2.06	1.39	53.71	46.59	0	Porphyry
73	MG4-2-2	134.19	52.53	2.55	2.63	42.56	2.32	1.79	54.62	43.82	1.56	Porphyry
74	MG4-2-5	133.68	52.52	2.55	2.74	62.84	3.46	2.81	54.62	43.82	1.56	Porphyry
75	MG4-4-2	135.60	52.59	2.58	2.60	54.99	2.83	2.37	54.62	43.82	1.56	Porphyry
76	MG4-4-3	135.61	52.57	2.58	2.74	57.69	3.15	2.64	54.62	43.82	1.56	Porphyry
77	MG4-6-3	136.47	52.59	2.59	2.65	49.25	2.61	2.02	54.62	43.82	1.56	Porphyry
78	MG4-8-3	135.53	52.62	2.58	2.73	47.85	2.59	1.90	67.61	29.98	2.42	Porphyry
79	MG4-8-5	135.58	52.63	2.58	2.72	52.82	2.66	2.21	67.61	29.98	2.42	Porphyry
80	MG5-2-1	133.33	52.03	2.56	2.64	24.26	1.60	1.87	89.07	8.51	2.42	Porphyry
81	MG5-3-2	134.17	52.49	2.56	2.48	22.31	1.54	1.81	70.22	24.26	5.52	Porphyry
82	MG5-3-3	138.19	52.58	2.63	2.49	22.14	1.35	1.59	70.22	24.26	5.52	Porphyry
83	MG5-3-4	134.28	52.54	2.56	2.52	20.95	0.59	1.30	70.22	24.26	5.52	Porphyry
84	MG5-4-6	135.21	52.63	2.57	2.24	19.23	0.53	0.96	70.22	24.26	5.52	Porphyry
85	MG5-4-9	134.29	52.48	2.56	2.26	16.35	0.49	0.73	70.22	24.26	5.52	Porphyry
86	MG5-4-11	135.61	52.23	2.60	2.23	15.58	0.44	0.69	89.07	8.51	2.42	Porphyry
87	MG5-5-6	136.21	52.64	2.59	2.58	30.28	2.13	2.98	14.96	76.60	8.44	Porphyry
88	MG5-5-7	137.10	52.63	2.60	2.49	22.62	1.73	2.55	14.96	76.60	8.44	Porphyry
89	MG5-5-8	135.71	52.63	2.58	2.53	20.90	1.59	1.74	14.96	76.60	8.44	Porphyry
90	MG5-5-10	136.25	52.65	2.59	2.51	18.60	1.02	1.13	14.96	76.60	8.44	Porphyry
91	MG5-5-5	136.85	52.68	2.60	2.53	33.19	2.17	3.71	14.96	76.60	8.44	Porphyry
92	MG5-6-6	136.22	52.63	2.59	2.45	22.38	1.73	2.46	26.56	70.77	2.66	Porphyry
93	MG5-6-7	130.84	52.62	2.49	2.52	25.68	1.82	2.70	26.56	70.77	2.66	Porphyry
94	MG5-6-9	136.04	52.57	2.59	2.51	21.99	1.71	2.08	26.56	70.77	2.66	Porphyry
95	MG5-8-2	135.02	53.82	2.51	2.59	26.55	2.00	2.88	39.81	60.19	0.00	Porphyry
96	MG5-8-6	135.26	53.77	2.52	2.60	30.95	2.14	3.21	39.81	60.19	0.00	Porphyry
97	MG5-9-4	135.47	53.03	2.55	2.61	28.60	2.01	2.96	26.56	70.77	2.66	Porphyry
98	MG5-9-A6	134.67	53.29	2.53	2.58	20.15	1.45	1.49	26.56	70.77	2.66	Porphyry
99	MG6-1-4	134.01	52.37	2.56	2.69	15.87	1.22	1.42	12.59	87.41	0.00	Porphyry
100	MG6-2-2	135.74	52.58	2.58	2.59	35.29	2.48	3.08	16.95	81.37	1.68	Porphyry
101	MG6-3-2	135.20	52.56	2.57	2.53	22.36	1.63	1.84	32.26	67.74	0.00	Porphyry
102	MG6-3-3	135.68	52.57	2.58	2.53	27.28	2.02	2.28	32.26	67.74	0.00	Porphyry
103	MG6-3-5	135.33	52.54	2.58	2.63	23.34	1.89	2.08	32.26	67.74	0.00	Porphyry
104	MG6-5-A1	135.46	52.64	2.57	2.73	34.84	2.25	2.82	12.59	87.41	0.00	Porphyry
105	MG6-6-1	135.05	52.63	2.57	2.73	44.60	3.07	3.54	23.12	76.88	0.00	Porphyry
106	MG6-7-6	135.39	53.75	2.52	2.75	30.89	2.17	2.70	23.12	76.88	0.00	Porphyry
107	MG6-7-7	135.46	53.78	2.52	2.58	42.66	2.86	3.33	23.12	76.88	0.00	Porphyry
108	MG6-7-8	136.60	53.80	2.54	2.78	38.38	2.64	3.12	23.12	76.88	0.00	Porphyry
109	MG6-10-11	136.31	54.16	2.52	2.67	28.71	2.04	2.34	10.59	88.41	1.10	Porphyry
110	MG6-10-12	134.92	54.03	2.50	2.66	26.93	1.99	2.26	10.59	88.41	1.10	Porphyry
111	MG11-1A-3	136.66	53.84	2.54	2.73	57.10	2.49	3.58	27.48	70.78	1.74	Porphyry
112	MG11-1A-6	132.02	53.84	2.45	2.73	48.87	2.27	2.61	27.48	70.78	1.74	Porphyry
113	MG11-2-1	134.96	53.86	2.51	2.60	43.46	2.80	2.73	27.48	70.78	1.74	Porphyry

Table B1 The results of UCTs, APLTs, DPLTs for 182 series of rock samples in saturated conditions (continued)

Row	Sample NO	L (mm)	d (mm)	L/d	$\rho_{(Sat)}$ (g/cm^3)	$UCS_{(Sat)}$ (MPa)	$I_{s(50)(Axial)(Sat)}$ (MPa)	$I_{s(50)(Diametral)(Sat)}$ (MPa)	Mineral composition			Texture
									GP	AN	CMs	
114	MG11-2-3	135.31	53.83	2.51	2.74	54.72	3.28	3.00	27.48	70.78	1.74	Porphyry
115	MG11-3-1	134.18	53.83	2.49	2.72	33.38	0.95	1.52	27.48	70.78	1.74	Porphyry
116	MG11-4-1	134.62	54.26	2.48	2.75	66.64	2.94	3.79	55.07	44.51	0.42	Porphyry
117	MG11-4-2	134.55	54.51	2.47	2.78	60.49	2.61	3.72	55.07	44.51	0.42	Porphyry
118	MG11-4-3	134.85	54.55	2.47	2.60	55.45	2.34	3.18	55.07	44.51	0.42	Porphyry
119	MG11-4-5	135.52	53.93	2.51	2.74	41.94	1.81	2.34	55.07	44.51	0.42	Porphyry
120	MG11-4-7	134.29	54.37	2.47	2.71	69.28	3.23	4.62	55.07	44.51	0.42	Porphyry
121	MG11-5-1	136.36	55.19	2.47	2.57	42.13	2.46	2.36	27.48	70.78	1.74	Porphyry
122	MG11-5-2	133.45	55.21	2.42	2.74	50.50	2.94	2.93	27.48	70.78	1.74	Porphyry
123	MG11-7-3	134.63	53.08	2.54	2.69	31.23	1.90	1.57	33.82	64.32	1.86	Porphyry
124	MG11-7-4	134.45	53.12	2.53	2.56	36.75	2.22	2.10	33.82	64.32	1.86	Porphyry
125	MG11-7-5	135.42	53.08	2.55	2.68	50.52	3.19	2.95	33.82	64.32	1.86	Porphyry
126	MG11-8-1	132.86	53.20	2.50	2.67	35.97	1.32	1.90	55.07	44.51	0.42	Porphyry
127	MG11-10-2	135.48	53.30	2.54	2.80	46.48	2.21	2.52	53.39	46.61	0.00	Porphyry
128	MG11-11-3	136.60	54.35	2.51	2.75	65.87	3.61	3.36	53.39	46.61	0.00	Porphyry
129	NG3-1-3	134.40	54.48	2.47	2.30	20.09	1.02	0.84	69.36	1.13	29.51	Alabaster
130	NG3-1-4	135.15	54.47	2.48	2.30	13.10	0.68	0.38	69.36	1.13	29.51	Alabaster
131	NG3-2-4	134.88	54.25	2.49	2.30	20.92	1.15	0.91	74.31	15.06	10.63	Alabaster
132	NG3-3-5	136.01	54.24	2.51	2.31	18.76	0.96	0.82	72.51	10.15	17.34	Alabaster
133	NG3-3-6	134.98	54.24	2.49	2.31	23.72	1.26	0.93	72.51	10.15	17.34	Alabaster
134	NG3-4-7	133.44	54.25	2.46	2.31	27.12	1.31	1.04	68.09	10.47	21.44	Alabaster
135	NG3-4-8	133.85	54.25	2.47	2.31	28.46	1.48	1.28	68.09	10.47	21.44	Alabaster
136	NG3-6-3	114.77	51.03	2.25	2.34	16.44	0.78	0.70	70.58	12.39	17.02	Alabaster
137	NG3-7-2	114.69	52.68	2.18	2.32	17.81	0.89	0.71	98.17	0.78	1.04	Alabaster
138	NG3-7-3	111.11	52.59	2.11	2.35	14.18	0.73	0.51	98.17	0.78	1.04	Alabaster
139	NG5-2-2	134.94	54.35	2.48	2.32	12.20	0.79	0.68	82.85	4.89	12.26	Alabaster
140	NG5-3-6	127.88	54.31	2.35	2.32	19.87	1.22	1.02	90.42	3.01	6.58	Alabaster
141	NG5-3-8	135.75	54.31	2.50	2.32	22.72	1.50	1.33	90.42	3.01	6.58	Alabaster
142	NG5-3-9	134.25	54.25	2.47	2.32	21.41	1.36	1.22	90.42	3.01	6.58	Alabaster
143	NG5-4-7A	118.70	54.44	2.18	2.30	10.71	0.57	0.60	88.87	1.86	9.27	Alabaster
144	NG5-5-2	135.47	54.19	2.50	2.31	16.72	1.21	1.03	42.60	54.03	3.37	Alabaster
145	NG5-5-6	135.57	54.21	2.50	2.31	16.03	0.93	0.73	42.60	54.03	3.37	Alabaster
146	NG5-5-7	131.86	54.21	2.43	2.31	20.41	1.85	1.65	42.60	54.03	3.37	Alabaster
147	NG5-5-9	135.28	54.21	2.50	2.32	22.83	2.13	1.82	42.60	54.03	3.37	Alabaster
148	NG5-5-10	129.54	54.30	2.39	2.31	18.08	1.42	1.22	42.60	54.03	3.37	Alabaster
149	NG5-6-5	120.88	54.47	2.22	2.30	14.55	1.00	0.81	84.91	0.64	14.45	Alabaster
150	NG5-7-8	125.74	54.55	2.31	2.31	18.03	1.15	0.95	88.87	1.86	9.27	Alabaster
151	NG5-8-5	134.14	54.52	2.46	2.30	15.84	1.12	0.90	80.67	7.61	11.72	Alabaster
152	NG5-8-6	136.00	54.69	2.49	2.30	13.05	0.82	0.76	80.67	7.61	11.72	Alabaster
153	NG5-8-7	134.44	54.61	2.46	2.30	10.07	0.54	0.57	80.67	7.61	11.72	Alabaster
154	NG5-9-A4	135.43	54.79	2.47	2.31	16.09	1.06	0.96	38.30	44.82	16.87	Alabaster
155	NG5-9-A5	135.11	54.82	2.46	2.31	18.75	1.67	1.44	38.30	44.82	16.87	Alabaster
156	NG5-9-B2	134.29	54.79	2.45	2.31	18.18	1.58	1.36	47.51	37.10	15.39	Alabaster
157	TG3-1-3	135.23	53.49	2.53	2.28	9.73	0.46	0.66	90.67	0.00	9.33	Alabaster
158	TG3-1-4	135.74	53.51	2.54	2.27	6.66	0.29	0.53	90.67	0.00	9.33	Alabaster

Table B1 The results of UCTs, APLTs, DPLTs for 182 series of rock samples in saturated conditions (continued)

Row	Sample NO	L (mm)	d (mm)	L/d	$\rho_{(Sat)}$ (g/cm^3)	$UCS_{(Sat)}$ (MPa)	$I_{s(50)(Axial)(Sat)}$ (MPa)	$I_{s(50)(Diametral)(Sat)}$ (MPa)	Mineral composition			Texture
									GP	AN	CMs	
159	TG3-2-2	135.25	53.44	2.53	2.30	11.98	0.54	0.72	98.00	0.00	2.00	Alabaster
160	TG3-2-3	134.98	53.42	2.53	2.30	15.61	0.75	0.91	98.00	0.00	2.00	Alabaster
161	TG3-3-5	134.61	53.64	2.51	2.28	14.30	0.72	0.90	90.67	0.00	9.33	Alabaster
162	TG3-3-6	134.95	53.59	2.52	2.29	13.48	0.56	0.75	90.67	0.00	9.33	Alabaster
163	TG3-3-7	135.17	53.53	2.53	2.28	11.44	0.47	0.69	90.67	0.00	9.33	Alabaster
164	TG3-5-5	135.75	53.54	2.54	2.31	17.93	0.96	1.53	94.00	4.00	2.00	Alabaster
165	TG3-5-6	129.33	53.54	2.42	2.32	21.40	1.26	1.98	94.00	4.00	2.00	Alabaster
166	TG3-9-4H	134.68	53.60	2.51	2.28	14.93	0.74	0.91	94.66	1.67	3.68	Alabaster
167	TG3-9-5H	134.68	53.56	2.51	2.30	13.83	0.67	0.78	94.66	1.67	3.68	Alabaster
168	TG3-9-8V	134.68	53.66	2.51	2.30	20.61	1.05	1.77	94.66	1.67	3.68	Alabaster
169	TG3-9-9V	135.77	53.66	2.53	2.30	16.75	0.78	1.04	94.66	1.67	3.68	Alabaster
170	TG3-10-1	135.72	52.90	2.57	2.29	16.90	0.87	1.06	98.00	0.00	2.00	Alabaster
171	TG4-1-4	134.43	53.47	2.51	2.29	20.29	1.27	0.74	86.41	2.90	10.69	Alabaster
172	TG4-1-5	135.79	53.45	2.54	2.29	11.67	0.58	0.57	86.41	2.90	10.69	Alabaster
173	TG4-1-6	135.44	53.54	2.53	2.29	13.88	0.81	0.61	86.41	2.90	10.69	Alabaster
174	TG4-1-7	134.78	53.47	2.52	2.29	23.10	1.36	0.89	86.41	2.90	10.69	Alabaster
175	TG4-6-2	133.48	53.58	2.49	2.30	27.62	1.57	0.98	97.00	0.00	3.00	Alabaster
176	TG4-7-4	129.73	52.76	2.46	2.30	10.91	0.39	0.28	96.33	1.00	2.67	Alabaster
177	TG10-3-3	120.60	53.58	2.25	2.27	19.64	1.15	0.70	84.41	3.88	9.71	Alabaster
178	TG10-3-4	134.28	54.36	2.47	2.26	19.27	1.07	0.62	84.41	3.88	9.71	Alabaster
179	TG10-6-2	120.49	53.87	2.24	2.29	11.08	0.46	0.48	96.33	0.00	4.67	Alabaster
180	TG10-6-3	124.06	53.80	2.31	2.29	12.74	0.72	0.59	96.33	0.00	4.67	Alabaster
181	TG10-8-2	128.04	53.96	2.37	2.30	17.01	0.92	0.61	82.01	8.68	9.31	Alabaster
182	TG10-10-3	134.58	53.88	2.50	2.31	9.61	0.37	0.19	97.33	0.00	2.67	Alabaster
Mean		133.34	53.45	2.50	2.42	24.02	1.35	1.49	63.30	26.37	10.33	
Max		138.61	55.21	2.63	3.31	69.28	3.61	4.62	98.17	88.41	35.39	
Min		111.11	51.03	2.11	0.00	2.56	0.16	0.19	10.59	0.00	0.00	
St.D		3.89	0.86	0.08	0.26	13.82	0.80	0.90	25.86	30.31	10.58	